BATCH: mp1a15 USER: ckt69 DIV: @xyv04/data1/CLS_pj/GRP_mp/JOB_i01/DIV_mp0500925 DATE: January 4, 2006

marrow, were first identified as bone-forming progenitor cells from rat marrow.[72] MSCs represent a very small fraction, 0.001−0.01% of the total population of nucleated cells in marrow.[73] They have the capacity to differentiate into cells of connective tissue lineages, including bone, fat, cartilage, and muscle. Recently, it has been reported that MSCs can differentiate into other lineages, such as neurons,[74] hepatocytes,[75] and insulin-producing cells.[76] Therefore, MSCs have attracted a great deal of interest because of their potential use in regenerative medicine and tissue engineering. To date, MSCs could be differentiated in vitro into proper lineages via a change in the culture conditions.[77] Another method for the in vitro differentiation is to genetically modify MSCs.[78,79] Although exogenous gene transfer into human MSCs (hMSCs) has been reported by using a conventional Ad vector, its transduction efficiency is quite low due to the scarcity of CAR.[80,81] Therefore, hMSCs have been transduced with high titers (more than 1000 infectious units/cell) of Ad vectors.[80,81] Fiber-modified Ad vectors have been applied for hMSCs to improve the transduction efficiency.[79,82,83] hMSCs infected with the AdRGD vector containing the BMP2 gene produced larger amounts of BMP2 than cells infected with the conventional Ad vector and efficiently differentiated into the osteogenic lineage.[82,83] Highly efficient transduction of hMSCs was achieved with tropism-modified Ad5 vectors carrying fiber shaft domains and knobs of different serotypes of Ad, such as Ad16, Ad35, or Ad50.[84] In a systematic comparison with various types of fiber-modified Ad vectors, the AdK7 vector is the most efficient for hMSCs and exhibited a 460-fold higher transduction efficiency than the conventional Ad vector.[79] The AdRGD vector or the Ad vector containing the Ad35 fiber (AdF35) exhibits a 16 or 130 times higher transduction efficiency, respectively, than the conventional Ad vector.[79] hMSCs are found to express CD46, which is the primary receptor for Ad35, but not CAR.[79] In conclusion, the AdK7 or AdF35 vector is the most appropriate for the transduction of hMSCs (Figure 3B).

Gene Transfer into Hematopoietic Stem Cells. Hematopoietic stem cells (HSCs) are capable of self-renewal and multilineage differentiation into all mature blood cells.[85] HSCs comprise only 0.01% of the whole bone marrow, the tissue in which they primarily reside.[86] Efficient transduction into HSCs would afford the opportunity to treat a number of hematopoietic disorders and would be a powerful tool for

(67) Chambers, I.; Colby, D.; Robertson, M.; Nichols, J.; Lee, S.; Tweedie, S.; Smith, A. Functional expression cloning of Nanog, a pluripotency sustaining factor in embryonic stem cells. *Cell* **2003**, *113*, 643−655.

(68) Kyba, M.; Perlingeiro, R. C.; Daley, G. Q. HoxB4 confers definitive lymphoid-myeloid engraftment potential on embryonic stem cell and yolk sac hematopoietic progenitors. *Cell* **2002**, *109*, 29−37.

(69) Antonchuk, J.; Sauvageau, G.; Humphries, R. K. HOXB4-induced expansion of adult hematopoietic stem cells ex vivo. *Cell* **2002**, *109*, 39−45.

(70) Blyszczuk, P.; Czyz, J.; Kania, G.; Wagner, M.; Roll, U.; St-Onge, L.; Wobus, A. M. Expression of Pax4 in embryonic stem cells promotes differentiation of nestin-positive progenitor and insulin-producing cells. *Proc. Natl. Acad. Sci. U.S.A.* **2003**, *100*, 998−1003.

(71) Kim, J. H.; Auerbach, J. M.; Rodriguez-Gomez, J. A.; Velasco, I.; Gavin, D.; Lumelsky, N.; Lee, S. H.; Nguyen, J.; Sanchez-Pernaute, R.; Bankiewicz, K.; McKay, R. Dopamine neurons derived from embryonic stem cells function in an animal model of Parkinson's disease. *Nature* **2002**, *418*, 50−56.

(72) Pittenger, M. F.; Mackay, A. M.; Beck, S. C.; Jaiswal, R. K.; Douglas, R.; Mosca, J. D.; Moorman, M. A.; Simonetti, D. W.; Craig, S.; Marshak, D. R. Multilineage potential of adult human mesenchymal stem cells. *Science* **1999**, *284*, 143−147.

(73) Pereira, R. F.; Halford, K. W.; O'Hara, M. D.; Leeper, D. B.; Sokolov, B. P.; Pollard, M. D.; Bagasra, O.; Prockop, D. J. Cultured adherent cells from marrow can serve as long-lasting precursor cells for bone, cartilage, and lung in irradiated mice. *Proc. Natl. Acad. Sci. U.S.A.* **1995**, *92*, 4857−4861.

(74) Sanchez-Ramos, J.; Song, S.; Cardozo-Pelaez, F.; Hazzi, C.; Stedeford, T.; Willing, A.; Freeman, T. B.; Saporta, S.; Janssen, W.; Patel, N.; Cooper, D. R.; Sanberg, P. R. Adult bone marrow stromal cells differentiate into neural cells in vitro. *Exp. Neurol.* **2000**, *164*, 247−256.

(75) Petersen, B. E.; Bowen, W. C.; Patrene, K. D.; Mars, W. M.; Sullivan, A. K.; Murase, N.; Boggs, S. S.; Greenberger, J. S.; Goff, J. P. Bone marrow as a potential source of hepatic oval cells. *Science* **1999**, *284*, 1168−1170.

(76) Hess, D.; Li, L.; Martin, M.; Sakano, S.; Hill, D.; Strutt, B.; Thyssen, S.; Gray, D. A.; Bhatia, M. Bone marrow-derived stem cells initiate pancreatic regeneration. *Nat. Biotechnol.* **2003**, *21*, 763−770.

(77) Kassem, M. Mesenchymal stem cells: Biological characteristics and potential clinical applications. *Cloning Stem Cells* **2004**, *6*, 369−374.

(78) Olmsted-Davis, E. A.; Gugala, Z.; Gannon, F. H.; Yotnda, P.; McAlhany, R. E.; Lindsey, R. W.; Davis, A. R. Use of a chimeric adenovirus vector enhances BMP2 production and bone formation. *Hum. Gene Ther.* **2002**, *13*, 1337−1347.

(79) Mizuguchi, H.; Sasaki, T.; Kawabata, K.; Sakurai, F.; Hayakawa, T. Fiber-modified adenovirus vectors mediate efficient gene transfer into undifferentiated and adipogenic-differentiated human mesenchymal stem cells. *Biochem. Biophys. Res. Commun.* **2005**, *332*, 1101−1106.

(80) Conget, P. A.; Minguell, J. J. Adenoviral-mediated gene transfer into ex vivo expanded human bone marrow mesenchymal progenitor cells. *Exp. Hematol.* **2000**, *28*, 382−390.

(81) Hung, S. C.; Lu, C. Y.; Shyue, S. K.; Liu, H. C.; Ho, L. L. Lineage differentiation-associated loss of adenoviral susceptibility and Coxsackie-adenovirus receptor expression in human mesenchymal stem cells. *Stem Cells* **2004**, *22*, 1321−1329.

(82) Tsuda, H.; Wada, T.; Ito, Y.; Uchida, H.; Dehari, H.; Nakamura, K.; Sasaki, K.; Kobune, M.; Yamashita, T.; Hamada, H. Efficient BMP2 gene transfer and bone formation of mesenchymal stem cells by a fiber-mutant adenoviral vector. *Mol. Ther.* **2003**, *7*, 354−365.

(83) Hamada, H.; Kobune, M.; Nakamura, K.; Kawano, Y.; Kato, K.; Honmou, O.; Houkin, K.; Matsunaga, T.; Niitsu, Y. Mesenchymal stem cells (MSC) as therapeutic cytoreagents for gene therapy. *Cancer Sci.* **2005**, *96*, 149−156.

(84) Knaan-Shanzer, S.; van de Watering, M. J.; van der Velde, I.; Goncalves, M. A.; Valerio, D.; de Vries, A. A. Endowing human adenovirus serotype 5 vectors with fiber domains of species B greatly enhances gene transfer into human mesenchymal stem cells. *Stem Cells* **2005**, *23*, 1598−1607.

(85) Weissman, I. L. Stem Cells: Units of development, units of regeneration, and units in evolution. *Cell* **2000**, *100*, 157−168.

the study of the proliferation, differentiation, and trafficking of HSCs. Although the retroviral and lentiviral transduction of HSCs to achieve stable gene expression has been established,[87,88] stable expression is not always desirable. For example, stable expression of MDR1 gene results in HSC expansion but can cause leukemia upon transplantation to recipient mice.[89] As the Ad vector mediates the exogenous gene expression transiently, this vehicle can be safe for gene therapy. However, the application of conventional Ad vectors for the transduction into human CD34+ cells, which contain a population of HSCs, has been limited because CAR is not expressed at sufficient levels in human CD34+ cells.[90,91] It has been shown that Ad serotype 35 (Ad35), which belongs to subgroup B, is efficient at binding to human CD34+ cells and hematopoietic cell lines.[90,92] We showed that the Ad35 vector, which is composed from the whole Ad35, achieved higher levels of transduction efficiency in human bone marrow CD34+ cells than both conventional Ad5 vectors and AdF35 vectors.[39,93] The expression level of reporter genes in the CD34+ cells transduced with the Ad35 vector was 12−76 and 1.4−3 times higher than that in the cells transduced with the Ad5 and AdF35 vectors, respectively.[39] The transduction efficiency of the Ad35 vector was slightly higher than that of the AdF35 vector, although the reason remains unknown. CD46 is ubiquitously expressed in almost all human cells, including human cord blood CD34+ cells.[94] Therefore, human CD34+ cells would be considered to be a suitable target for the Ad35 vector (Figure 3C). As a result of the systematic comparison of promoters with Ad35 vectors, significantly higher transduction efficiencies were achieved with the EF-1α, CA, and CMV promoter/enhancer with the largest intron of CMV (intron A) (CMVi) promoters. In particular, the CA promoter was found to allow for the highest transduction efficiencies in both the whole human CD34+ cells and the immature subsets.[93] In mice, a population of mouse bone marrow highly enriched for HSC, called side population (SP) cells, has been reported to be transduced with the conventional Ad5 vector.[95] This suggests that pure mouse HSCs might express CAR on the cell surface. Further studies are needed to clarify this. The Ad vector-mediated transduction of hematopoietic regulator genes, such as HoxB4,[68,69] Bmi-1,[96] or SCL/Tal-1,[97] into HSCs may be effective for therapeutic use such as HSC expansion, although the Ad vector expressing HoxB4 was unsuccessful because of unexpected HSC differentiation due to its high transduction efficiency.[98]

Conclusions

We have reviewed recent advances in the development of improved Ad vectors for stem cells. Ad vectors have advantages over other viral vectors: the high transduction efficiency, the ease of vector preparation, and the transient expression ability. By the Ad vector-mediated introduction of a differentiation master regulator gene, we could control the differentiation of stem cells. These technical advances should greatly facilitate the analysis of gene function in the stem cells as well as the therapeutic applications of gene-modified stem cells.

Abbreviations Used

ES, embryonic stem; mES, mouse ES; MSCs, mesenchymal stem cells; HSCs, hematopoietic stem cells; Ad, adenovirus; CAR, coxsackievirus and adenovirus receptor; Ad5, Ad serotype 5; ITR, inverted terminal repeats; Ad35, Ad serotype 35; AdRGD vector, Ad vector containing the RGD

(86) Morrison, S. J.; Weissman, I. L. The long-term repopulating subset of hematopoietic stem cells is deterministic and isolatable by phenotype. *Immunity* **1994**, *1*, 661−673.

(87) Dao, M. A.; Shah, A. J.; Crooks, G. M.; Nolta, J. A. Engraftment and retroviral marking of CD34+ and CD34+CD38- human hematopoietic progenitors assessed in immune-deficient mice. *Blood* **1998**, *91*, 1243−1255.

(88) Sirven, A.; Ravet, E.; Charneau, P.; Zennou, V.; Coulombel, L.; Guetard, D.; Pflumio, F.; Dubart-Kupperschmitt, A. Enhanced transgene expression in cord blood CD34(+)-derived hematopoietic cells, including developing T cells and NOD/SCID mouse repopulating cells, following transduction with modified trip lentiviral vectors. *Mol. Ther.* **2001**, *3*, 438−448.

(89) Bunting, K. D.; Galipeau, J.; Topham, D.; Benaim, E.; Sorrentino, B. P. Transduction of murine bone marrow cells with an MDR1 vector enables ex vivo stem cell expansion, but these expanded grafts cause a myeloproliferative syndrome in transplanted mice. *Blood* **1998**, *92*, 2269−2279.

(90) Shayakhmetov, D. M.; Papayannopoulou, T.; Stamatoyannopoulos, G.; Lieber, A. Efficient gene transfer into human CD34(+) cells by a retargeted adenovirus vector. *J. Virol.* **2000**, *74*, 2567−2583.

(91) Rebel, V. I.; Hartnett, S.; Denham, J.; Chan, M.; Finberg, R.; Sieff, C. A. Maturation and lineage-specific expression of the coxsackie and adenovirus receptor in hematopoietic cells. *Stem Cells* **2000**, *18*, 176−182.

(92) Segerman, A.; Mei, Y. F.; Wadell, G. Adenovirus types 11p and 35p show high binding efficiencies for committed hematopoietic cell lines and are infective to these cell lines. *J. Virol.* **2000**, *74*, 1457−1467.

(93) Sakurai, F.; Kawabata, K.; Yamaguchi, T.; Hayakawa, T.; Mizuguchi, H. Optimization of adenovirus serotype 35 vectors for efficient transduction in human hematopoietic progenitors: Comparison of promoter activities. *Gene Ther.* **2005**, *12*, 1424−1433.

(94) Manchester, M.; Smith, K. A.; Eto, D. S.; Perkin, H. B.; Torbett, B. E. Targeting and hematopoietic suppression of human CD34+ cells by measles virus. *J. Virol.* **2002**, *76*, 6636−6642.

(95) Bradfute, S. B.; Goodell, M. A. Adenoviral transduction of mouse hematopoietic stem cells. *Mol. Ther.* **2003**, *7*, 334−340.

(96) Park, I. K.; Qian, D.; Kiel, M.; Becker, M. W.; Pihalja, M.; Weissman, I. L.; Morrison, S. J.; Clarke, M. F. Bmi-1 is required for maintenance of adult self-renewing haematopoietic stem cells. *Nature* **2003**, *423*, 302−305.

(97) Porcher, C.; Swat, W.; Rockwell, K.; Fujiwara, Y.; Alt, F. W.; Orkin, S. H. The T cell leukemia oncoprotein SCL/tal-1 is essential for development of all hematopoietic lineages. *Cell* **1996**, *86*, 47−57.

(98) Brun, A. C.; Fan, X.; Bjornsson, J. M.; Humphries, R. K.; Karlsson, S. Enforced adenoviral vector-mediated expression of HOXB4 in human umbilical cord blood CD34+ cells promotes myeloid differentiation but not proliferation. *Mol. Ther.* **2003**, *8*, 618−628.

peptide; Ad K7 vector, Ad vector containing a polylysine stretch; hES, human ES; STAT3, signal transducer and activator of transcription 3; LIF, leukemia inhibitory factor; STAT3F, dominant-negative mutant of STAT3; hMSCs, human MSCs; BMP2, bone morphogenetic protein 2; AdF35, Ad vector containing the Ad35 fiber.

MP0500925

Journal: Gt | Disk used | Despatch Date: 10/2/2006
Article : npg_gt_3302749 | Pages: 1–9 | OP: Deeparani ED: Indira

Gene Therapy (2006) 0, 1–9
© 2006 Nature Publishing Group All rights reserved 0969-7128/06 $30.00
www.nature.com/gt

SHORT COMMUNICATION

Adenovirus serotype 35 vector-mediated transduction into human CD46-transgenic mice

F Sakurai[1], K Kawabata[1], N Koizumi[1], N Inoue[2], M Okabe[2], T Yamaguchi[3], T Hayakawa[4] and H Mizuguchi[1,5]

[1]*Laboratory of Gene Transfer and Regulation, National Institute of Biomedical Innovation, Osaka, Japan;* [2]*Genomic Information Research Center, Osaka University, Osaka, Japan;* [3]*Division of Cellular and Gene Therapy Products, National Institute of Health Sciences, Tokyo, Japan;* [4]*Pharmaceuticals and Medical Devices Agency, Tokyo, Japan and* [5]*Graduate School of Pharmaceutical Sciences, Osaka University, Osaka, Japan*

We previously demonstrated that systemic administration of adenovirus serotype 35 (Ad35) vectors to mice does not mediate efficient transduction in organs, probably because expression of the mouse analog of the subgroup B Ad receptor, human CD46 (membrane cofactor protein), is limited to the testis. Here, we describe the in vitro *and* in vivo *transduction characteristics of Ad35 vectors by using homozygous and hemizygous human CD46 transgenic (CD46TG) mice, which ubiquitously express human CD46. An Ad35 vector more efficiently transduced the primary dendritic cells and macrophages prepared from CD46TG mice than those from wild-type mice.* In vivo *transduction experiments demonstrated that CD46TG mice are more susceptible to Ad35 vector-mediated* in vivo *transduction than are wild-type mice. In particular, homozygous CD46TG mice, which express higher levels of CD46 in the organs than hemizygous CD46TG mice, tend to exhibit higher transduction efficiencies after intraperitoneal administration than hemizygous CD46TG mice. Intraperitoneal administration of Ad35 vectors resulted in efficient transduction into the mesothelial cells of the peritoneal organs in homozygous CD46TG mice. These results indicate that an Ad35 vector recognizes human CD46 as a cellular receptor in CD46TG mice. However, the* in vivo *transduction efficiencies of Ad35 vectors in CD46TG mice are much lower than those of conventional Ad5 vectors in wild-type mice.*
Gene Therapy (2006) **0,** 000–000. doi:10.1038/sj.gt.3302749

Keywords: *adenovirus serotype 35 vector, human CD46, human CD46-transgenic mice, receptor, biodistribution, gene therapy*

The human adenoviruses (Ads) comprise a group of 51 serologically distinct viruses.[1,2] Among them, Ad vectors widely used for gene therapy are based on Ad serotype 5 (Ad5), which belongs to subgroup C. Ad5 vectors have several attractive features as gene delivery vehicles; for example, they have noteworthy *in vivo* transduction efficiency and transduction ability into both proliferating and non-proliferating cells. In addition, Ad5 vectors can be grown to high titer, and large stretches of foreign DNA can be inserted into the Ad5 vector genome.

However, recent studies have revealed several disadvantages associated with the clinical use of Ad5 vectors. One disadvantage is the high prevalence of adult humans (>50%) that produce neutralizing antibodies to Ad5.[3,4] Preexisting neutralizing antibodies prevent Ad vectors from transducing cells *in vivo*.[5] Furthermore, Ad vector preimmunization in mice has been demonstrated to significantly increase vector-mediated liver toxicity on re-exposure.[6] Therefore, preexisting immunity to Ad5 vectors greatly hampers the *in vivo* application of Ad5 vectors. Inefficient transduction with Ad5 vectors of cells lacking expression of a primary receptor for Ad5, coxsackievirus and adenovirus receptor (CAR), also is highly problematic. Several important target cells for gene therapy, including hematopoietic stem cells,[7] dendritic cells[8] and malignant tumor cells,[9] express low levels of CAR.

To overcome these drawbacks of Ad5 vectors, several groups (including ours) have developed Ad vectors composed of other human Ad serotypes, such as Ad serotype 7a,[10] 11,[4,11] and 35,[12–15] and Ads of animal origin, such as chimpanzee,[16] bovine,[17] mouse,[18] and ovine.[19] Among these non-Ad5 vectors, those composed of human Ad11 and Ad35, which belong to subgroup B, are highly promising as gene transfer vectors for the following reasons. First, Ad11 and Ad35 are serotypes least neutralized by serum from healthy human blood donors: less than 20% of serum samples are positive for anti-Ad11 and -Ad35 neutralizing antibodies.[14] Second, human subgroup B Ads, including Ad11 and Ad35, recognize human CD46 (membrane cofactor protein) as a cellular receptor,[20,21] although Ads belonging to subgroups A, C, D, E, and F use CAR as a primary receptor. CD46 is a single-chain type I transmembrane glycoprotein that is ubiquitously expressed in all cells (except

Correspondence: Dr H Mizuguchi, Laboratory of Gene Transfer and Regulation, National Institute of Biomedical Innovation, 7-6-8 Asagi, Saito, Ibaragi-City, Osaka 567-0085, Japan.
E-mail: mizuguch@nibio.go.jp
Received 29 September 2005; revised 19 January 2006; accepted 21 January 2005

erythrocytes) in humans, suggesting that human subgroup B Ads can infect almost all human cell types, regardless of CAR expression. We previously demonstrated that Ad35 vectors show broad tropism toward human cells,[12,13,22] including CAR-negative cells, because of the ubiquitous expression of CD46. Furthermore, CD46 expression is highly upregulated in human malignant tumor cells,[23,24] suggesting that these cells would be suitable targets for Ad35 vector-mediated transduction.

Ad35 vectors exhibit efficient transduction in a variety of human cells *in vitro*. In contrast, systemic administration of Ad35 vectors into mice mediates low levels of transduction efficiencies in organs.[13,14] The refractoriness of mice to Ad35 vectors would be due to the expression pattern of CD46 in this host. Whereas CD46 is ubiquitously expressed in humans, expression of mouse CD46 is limited to the testes. In addition, mouse and human CD46s are only 46% similar.[25] These differences indicate that the conventional mouse is not a suitable small animal model for characterization of Ad35 vector-mediated *in vivo* transduction. A small animal model in which the transduction properties of Ad35 vectors can be characterized appropriately is essential to estimate the efficiency of Ad35 vector-mediated transduction in humans.

In the present study, to evaluate the *in vivo* transduction properties of Ad35 vectors in an animal model that ubiquitously expresses CD46 (as do humans), we administered Ad35 vectors intravenously and intraperitoneally into homozygous and hemizygous human CD46-transgenic (CD46TG) mice, which have a human CD46 gene inserted into the mouse genome. Our results indicate that CD46 acts as an attachment receptor for Ad35 after *in vivo* administration, but the transduction efficiencies in organs were lower than we had expected.

First, Western blot analysis was performed to examine human CD46 expression levels in the organs of homozygous and hemizygous CD46TG mice. As shown in Figure 1, human CD46 was ubiquitously expressed in all organs examined of homozygous and hemizygous CD46TG mice. In particular, amounts of CD46 were higher in the liver, spleen, lung, and kidney than in other organs. CD46 expression patterns in CD46TG mice mimicked those observed in humans, which were reported previously,[26] and homozygous CD46TG mice expressed CD46 more abundantly than hemizygous mice. CD46 expression in the liver, spleen, and diaphragm of homozygous mice was 3.2, 3.7, and 3.2 times that, respectively, in these organs of the hemizygous mice. We also confirmed that human CD46 expression levels in the primary hepatocytes, splenocytes, and thymocytes of the homozygous mice were similar to, or lower than, those in human cultured cell lines (human hepatoma and leukemia lines; data not shown). Flow cytometric and Western blotting analysis failed to detect CD46 expression in the erythrocytes of our CD46TG mice (data not shown), although detectable levels of CD46 were expressed in the erythrocytes of some CD46TG mice lines used in other studies.[27,28]

Next, we performed *in vitro* transduction of an Ad35 vector into bone marrow-derived dendritic cells (mBM-DC) and peritoneal macrophages prepared from CD46TG and wild-type mice. Recently, the potential utility of Ad35 vectors as vaccine vectors has been proposed,[29,30] and DC and macrophages are considered to be ideal targets for immunotherapy using Ad35 vector-based vaccines. mBM-DC[31] and peritoneal macro-

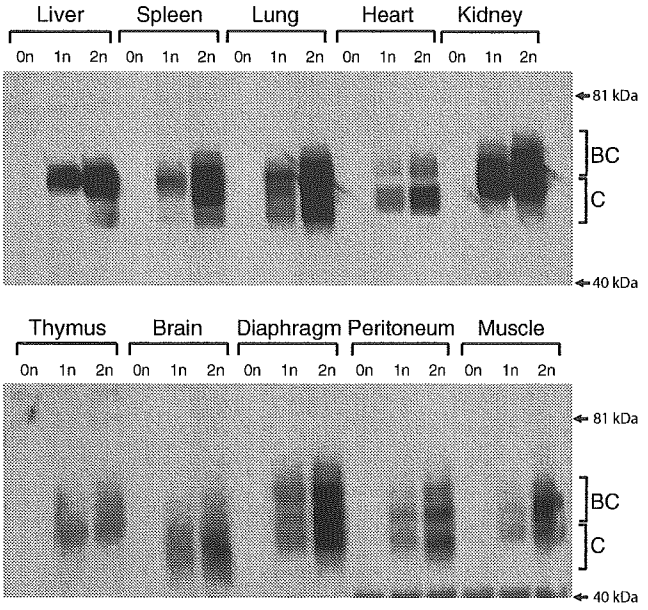

Figure 1 Human CD46 expression in organs harvested from CD46TG mice. The protein samples were prepared from wild-type mice (0n), hemizygous CD46TG mice (1n), and homozygous CD46TG mice (2n). The molecular masses of marker proteins (kDa) and approximate positions of the two major isoforms of the CD46 proteins (BC and C isoforms) are indicated on the right. CD46TG mice were produced as follows. Spermatozoa were dispersed from the epididymis of mature (>12 weeks old) B6D2F1 male mice into 400 μl of TYH medium[50] and were frozen in liquid nitrogen immediately after dilution with TYH medium to 1×10^7/ml. The bacterial artificial chromosome (BAC) DNA carrying human CD46 (5 μg/ml in TE) (GenomeSystems Inc., St Louis, MO) was added to thawed sperm after purification by using Large-Construct Kit (Qiagen, Valencia, CA). The mixture was incubated for 5 min at room temperature and then diluted by 9 volumes of 12% PVP-HCZB. Metaphase II oocytes for microinjection were prepared from B6D2F1 female mice, as described previously.[51] These oocytes were maintained in potassium simplex optimized medium (kSOM) under mineral oil equilibrated in 5% (v/v) CO_2 in air at 37°C until use. For microinjection, sperm heads were aspirated into a pipette attached to a piezoelectric pipette-driving unit, and a sperm head was injected into each oocyte, as described previously.[51] After injection, the eggs were incubated in kSOM until 2-cell stage, and were transferred to ICR pseudopregnant foster mothers. CD46TG mice were detected among the pups born by using genomic PCR as described previously.[40] After backcrossing to the C57Bl6 background for more than five generations, homozygous CD46TG mice were obtained by mating hemizygous mice. Homozygous CD46TG mice were identified by mating CD46TG mice with wild-type mice. For Western blotting analysis, organs collected from wild-type mice (C57Bl6, female, 5 weeks old, obtained from Nippon SLC Co. Ltd., Shizuoka, Japan) and CD46TG mice (female, 5 weeks old) were homogenized in phosphate buffered saline (PBS) buffer containing 1% Triton-X, 2 mM EGTA, and proteinase inhibitor cocktail (1 mM PMSF, 1 μg/ml pepstatin, and 1 μg/ml leupeptin). After centrifugation of the homogenates, the supernatants (7.5 μg protein per sample) underwent nonreducing sodium dodecyl sulfate-12.5% polyacrylamide gel electrophoresis, and the separated proteins were transferred to a nitrocellulose membrane. After blocking of nonspecific binding, CD46 was detected with anti-CD46 rabbit serum (1:5000; kindly provided by Dr T Seya, Hokkaido University, Japan), followed by incubation in the presence of peroxidase-labeled anti-rabbit antibody (1:6000). Signals on the membrane was visualized and analyzed as described previsouly.[52]

phages[32] were prepared as described previously. An Ad35 vector that expresses green fluorescence protein (GFP), Ad35GFP, was prepared by means of an improved *in vitro* ligation method[22,33,34] using 293-E1B cells as a packaging cell line. 293-E1B cells are stable transformants expressing Ad35E1B proteins, which were generated by transfection of pEF-Ad35E1B into 293 cells and after selection with G418 (Invitrogen, Carlsbad, CA, USA). pEF-Ad35E1B was constructed by insertion of the fragment of the Ad35 genome (bp 1911–3413), which contains the Ad35 E1B-55 K gene, into pEF/myc/nuc (Invitrogen). The plaque forming unit (PFU)-to-particle ratios of Ad35GFP in 293-E1B cells was 1:66.

Flow cytometric analysis showed that mBM-DC from hemizygous and homozygous CD46TG mice express considerable amounts of human CD46 (Figure 2a): 47% of the mBM-DC from hemizygous mice and 87% of those from homozygous mice were CD46-positive (% of M1-gated). Transduction experiments demonstrated that Ad35GFP mediated more efficient transduction in mBM-DC from CD46TG mice than from wild-type mice (Figure 3a). Ad35GFP at a dose of 3000 vector particles (VP)/cell successfully transduced about 42% of the mBM-DC from the hemizygous CD46TG mice and 83% of those from homozygous mice. In contrast, only 3.8% of the mBM-DC from wild-type mice were positive for GFP expression, a rate that is only slightly above background level. In addition, mean fluorescence intensity data revealed that the mBM-DC from CD46TG mice were more susceptible to Ad35 vector than those from wild-type mice. Similar results were obtained for peritoneal macrophages. Human CD46 was expressed in 20% of the peritoneal macrophages from hemizygous CD46TG mice and in 41% of those from homozygous animals (Figure 2b). Infection by Ad35GFP resulted in 10% GFP-positive macrophages from hemizygous CD46TG mice and in 20% GFP-positive macrophages among those from homozygous transgenic mice. In contrast, the macrophages from wild-type mice were refractory to Ad35 vector-mediated transduction (Figure 3b). These results indicate that human CD46 expression greatly increases the transduction efficiency of Ad35 vector in mouse primary cells and that the *in vitro* transduction efficiency of Ad35 vector depended on CD46 expression density.

The refractoriness of mBM-DC and macrophages from wild-type mice also suggests inefficient interaction between the RGD motif in the penton base of Ad35 vector and αv-integrins on the cells. The hypervariable RGD loop in the penton base of the Ad35 vector is supposed to be shorter than that of conventional Ad5 viruses because the RGD loop of Ad serotype 11 (55 amino acids), which sequence is identical to that of Ad35, is shorter than that of Ad2 (74 amino acids).[35] It suggests that αv-integrins on the cell surface might be less easily accessible to the RGD motif in the penton bases of Ad35 viruses, compared with Ad5 vectors. To varying degrees, conventional Ad5 vectors transduce via interaction between the RGD motif in the penton base and αv-

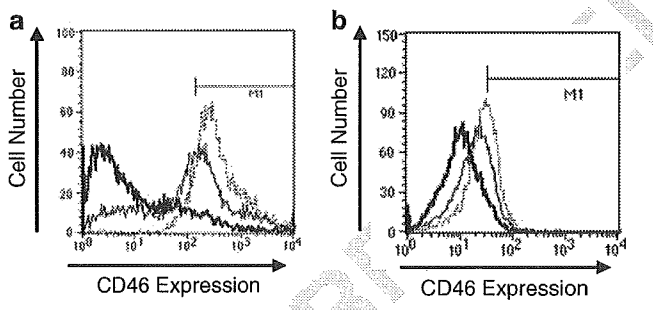

	% of M1-gated
Wild-type	8.2 %
Hemi TG	46.6 %
Homo TG	86.6 %

	% of M1-gated
Wild-type	5.0 %
Hemi TG	19.8 %
Homo TG	40.5 %

Figure 2 CD46 expression in (**a**) mBM-DC and (**b**) peritoneal macrophages from wild-type mice and CD46TG mice. Thick lines, thin lines, and dotted lines represent cells from wild-type mice (C57Bl6, 5 weeks old), and hemizygous (Hemi TG, 5–6 weeks old), and homozygous (Homo TG, 5–6 weeks old) CD46TG mice, respectively. mBM-DC and peritoneal macrophages were incubated with fluorescein isothiocyanate (FITC)-conjugated anti-human CD46 antibody (E4.3; Pharmingen, San Diego, CA) after incubation with anti-FcγRII/III monoclonal antibody (2.4G2; Pharmingen) to block nonspecific binding of the anti-human CD46 antibody. After being washed thoroughly, 10^4 stained cells were analyzed using a FACSCalibur (Becton Dickinson, Tokyo, Japan) and CellQuest software (Becton Dickinson).

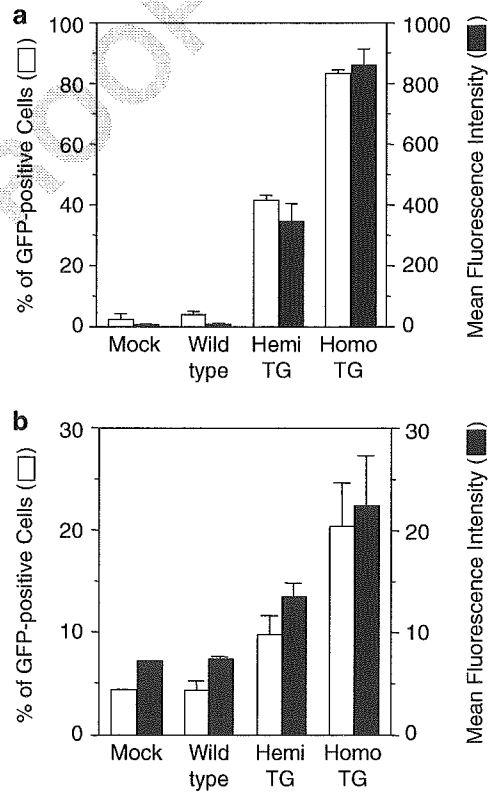

Figure 3 Ad35 vector-mediated GFP expression in (**a**) mBM-DC and (**b**) peritoneal macrophages prepared from wild-type mice and CD46TG mice. Open bars represent percentages of cells positive for GFP, and closed bars indicate mean fluorescence intensity. mBM-DC (5×10^5 cells/well) and peritoneal macrophages (2×10^5 cells/well) prepared from wild-type mice and hemizygous (Hemi TG) and homozygous (Homo TG) CD46TG mice were seeded into 12-well plates the day before transduction. The cells then were transduced with Ad35GFP at 3000 VP/cell for 1.5 h. After a total of 48 h of incubation, GFP expression in cells was evaluated by flow cytometric analysis. The results are represented as mean ± s.d. ($n = 3$).

UNCORRECTED PROOF

integrins, even in the absence of the primary receptor for Ad5, CAR.[36]

Next, to assess the *in vivo* transduction properties of Ad35 vectors in CD46TG mice, we intravenously and intraperitoneally administered an Ad35 vector that expressed luciferase (Ad35L). Ad35L was prepared in the same way as Ad35GFP. The PFU-to-particle ratio of Ad35L in 293-E1B cells was 1:625. Intravenous administration of Ad35L to hemizygous and homozygous CD46TG mice increased the transduction efficiencies for the liver, lung, and kidney over those in wild-type mice. In contrast, no apparent increase in luciferase production occurred in the spleen or thymus of CD46TG mice (Figure 4a). There were no clear differences in the transduction efficiencies of Ad35 vectors between the homozygous and hemizygous mice, except in the case of liver.

In contrast, transduction efficiencies of Ad35L in the liver, spleen, and kidney of CD46TG mice after intraperitoneal administration were much higher than those after intravenous administration (Figure 4b). Intraperitoneal injection into homozygous mice led to transduction efficiencies in the liver and kidney that were 83 and 271 times that after intravenous administration, respectively. Furthermore, even larger differences in transduction efficiency occurred between CD46TG mice and wild-type mice after intraperitoneal injection. Luciferase production from the liver, kidney, and diaphragm of homozygous mice was 536, 492, and 83 times, respectively, that of wild-type mice. Comparison of the homozygous and hemizygous mice demonstrated that after intraperitoneal administration of vector, the homozygous mice appeared to be more susceptible to Ad35 vectors. Transgene expression levels in the liver and diaphragm of homozygous mice were 6.8 and 5.5 times, respectively, those of the hemizygous mice. The increased transduction efficiencies in the homozygous mice probably are due to their increased levels of CD46 expression (Figure 1). These results indicate that CD46TG mice are more susceptible to Ad35 vectors than wild-type mice. However, the transduction efficiencies of Ad35 vectors in CD46TG mice after both intraperitoneal and intravenous injection were much lower than those of conventional Ad5 vectors in wild-type mice.[13] Luciferase production in the liver and spleen by Ad35 vectors intravenously administered to homozygous CD46TG mice was 20000 and 57 times lower, respectively, than that from Ad5 vectors administered intravenously to wild-type mice at the same dose as for the Ad35 vector in the present study (Ad5 vector-mediated luciferase expression levels in wild-type mice at a dose of 1.5×10^{10} VP/mouse after intravenous administration: liver, 2266 pg/mg protein; spleen, 0.893 pg/mg protein; kidney, 0.768 pg/mg protein; heart, 2.13 pg/mg protein; lung, 0.252 pg/mg protein).[13]

Next, to compare the fate of Ad35 vectors after *in vivo* administration to wild-type versus CD46TG mice, we used real-time PCR at 48 h post-administration to measure the amounts of Ad35L genomic sequences that had accumulated in various organs. After intravenous administration to CD46TG mice, the vector DNA in the sampled organs of CD46TG mice (except for liver) exceeded that in those of wild-type mice (Figure 5a). In addition, homozygous mice appeared to take up higher amounts of Ad35L than hemizygous mice. For example,

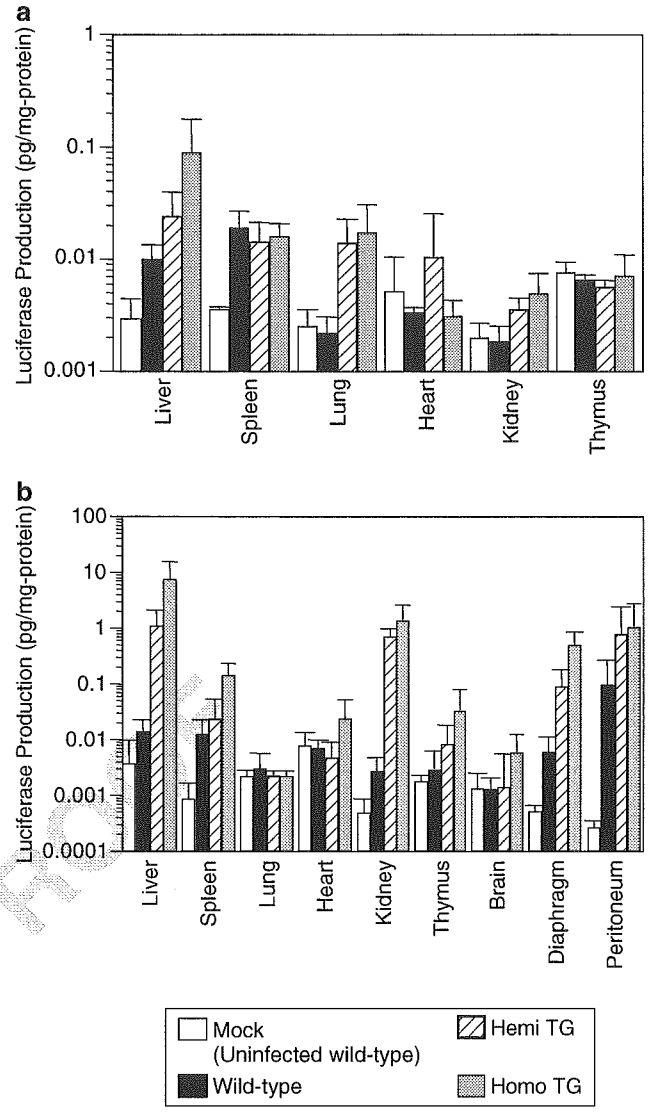

Figure 4 Luciferase production in CD46TG and wild-type mice after intravenous and intraperitoneal administration of Ad35L. (**a**) Luciferase production after intravenous administration of the vector. (**b**) Luciferase production after intraperitoneal administration. Ad35L (1.5×10^{10} VP) was administered to wild-type mice (C57Bl6, 5 weeks old) and hemizygous (Hemi TG, 5–6 weeks old) and homozygous (Homo TG, 5–6 weeks old) CD46TG mice. After 48 h, the organs were harvested and homogenized as described previously,[53] and luciferase production was measured by a luminescence assay system (PicaGene 5500; Toyo Inki, Japan). All data are represented as mean ± s.d. ($n = 4$, intravenous administration; $n = 6$, intraperitoneal administration).

Ad35 vector quantities in the spleen, which contained the most Ad35 vector DNA among the organs tested, of hemizygous and homozygous mice were 8 and 69 times, respectively, that in wild-type mice. In contrast, Ad35 vector DNA did not accumulate to high levels in the liver of CD46TG mice. Moreover, these quantities were similar, or slightly lower than, those in other organs of CD46TG mice, even though liver is well known to be a predominant organ for sequestration of Ad5 vectors administered intravenously to mice.[37,38]

After intraperitoneal injection, Ad35L was accumulated more efficiently in the liver, kidney, peritoneum,

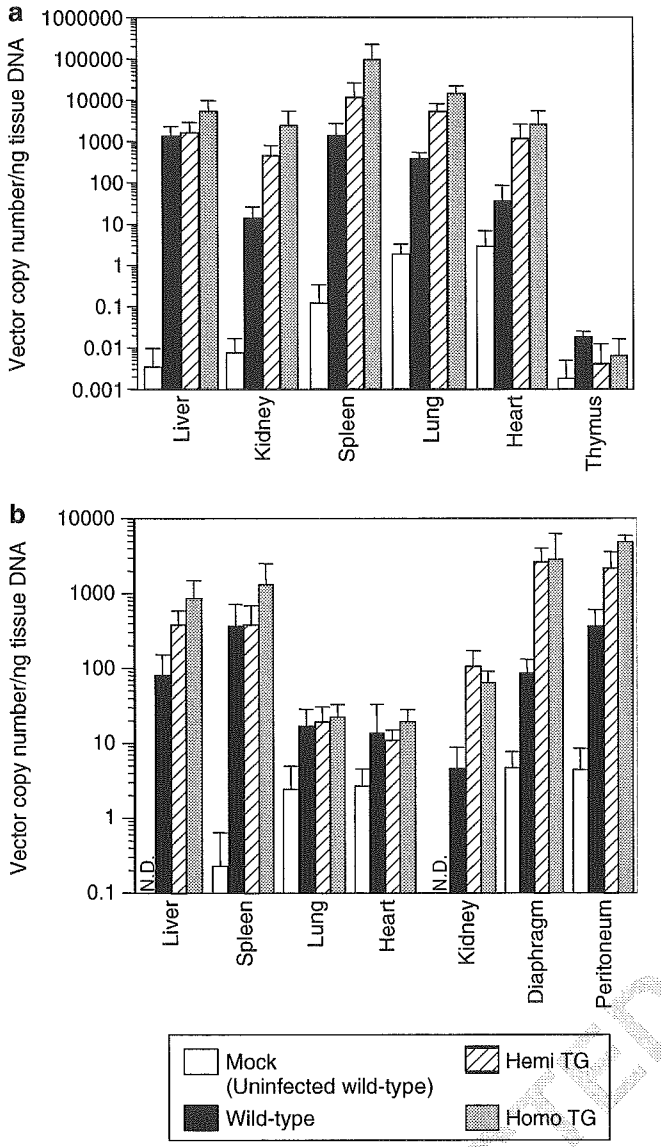

Figure 5 Tissue distribution of viral DNA in CD46TG and wild-type mice after intravenous and intraperitoneal administration of Ad35L. (**a**) Ad35L vector DNA detected in organs after intravenous administration. (**b**) Ad35L vector DNA detected in organs after intraperitoneal administration. Ad35L (1.5×10^{10} VP) was administered to wild-type mice (C57Bl6, 5 weeks old) and hemizygous (Hemi TG, 5–6 weeks old) and homozygous (Homo TG, 5–6 weeks old) CD46TG mice. After 48 h, the organs were harvested, and total DNA including viral DNA was extracted from the tissues after proteinase K digestion, and 25-ng samples of total DNA were subjected to quantitative real-time PCR, as described previously.[22] The data are represented as mean ± s.d. ($n = 4$).

and diaphragm of CD46TG mice than in those organs of wild-type mice (Figure 5b). The quantities of vector DNA in the liver and kidney of homozygous CD46TG mice were 11 and 14 times, respectively, those of wild-type mice. Furthermore, Ad35 vector DNA tended to be accumulated more efficiently in the liver, spleen, peritoneum, and diaphragm of the homozygous mice than in these organs of the hemizygous mice. In addition, low levels of viral DNA were detected in the lung and heart, which are not directly accessible to intraperitoneally injected Ad35L from the injection point, with no significant difference between CD46TG mice and wild-type mice in the amounts that were detected. The data on the *in vivo* transduction efficiencies and viral DNA accumulation indicate that Ad35 vectors administered *in vivo* use human CD46 in CD46TG mice. In both intravenous and intraperitoneal dosing experiments, the total amounts of Ad35 vector DNA recovered from wild-type mice were lower than those from CD46TG mice. The decreased recovery of Ad35 vector DNA from wild-type mice could be due to its degradation in phagocytic cells, such as liver Kupffer cells. We speculate that the absence of human CD46 expression in organs results in decreased infection of the organs and increased uptake of Ad35 vector by phagocytic cells, leading to degradation of Ad35 vector DNA. In the previous study, we demonstrated that Ad35 vectors predominantly were taken up by liver nonparenchymal cells (endothelial and Kupffer cells) after intravenous administration in wild-type mice and that the internalized Ad35 vector DNA was degraded rapidly.[13]

Finally, to examine the types of cells that Ad35 vectors transduce in CD46TG mice, we performed X-gal staining of the peritoneal organs after intraperitoneal administration of Ad35LacZ, an Ad35 vector expressing β-galactosidase (dose, 7.5×10^{10} VP/mouse). The vector was prepared by means of an improved *in vitro* ligation method[22,33,34] using pAdMS18 and pHMCMV6-LacZ. pAdMS18 was constructed by ligating oligonucleotides encoding I-*Ceu*I/*Swa*I/PI-*Sce*I into the *Pac*I site of pFS2-Ad35–7.[12] pHMCMV6-LacZ was generated by cloning the *Escherichia coli* β-galactosidase gene derived from pCMVβ (Clontech, Palo Alto, CA) into the multicloning site of pHMCMV6.[34] The PFU-to-particle ratio of Ad35LacZ in 293-E1B cells was 1:315.

The peritoneal organs (liver, kidney, and peritoneum) were efficiently transduced with Ad35LacZ (Figure 6a–f). However, X-gal staining of liver and kidney sections revealed that mainly the mesothelial cells on the surface of the liver and kidney were transduced; few deeper cells were transduced (Figure 6g–j). These results indicate that after injection, Ad35 vectors directly access the mesothelial cells of these organs, leading to efficient transduction.

In the present study, we assessed the *in vitro* and *in vivo* transduction properties of Ad35 vectors by using homozygous and hemizygous human CD46TG mice, a small animal model in which human CD46 is expressed with human-like tissue specificity. Human CD46 serves as a cellular receptor for not only subgroup B Ads but also several human pathogens, including measles virus, human herpes virus 6, and two types of bacteria.[39] Therefore, CD46TG mice already have been used in several studies, which have reported that replication of the pathogens and inflammatory responses occur in CD46TG mice after exposure to the pathogens, demonstrating the utility of CD46TG mice as animal models (note that for study of measles virus, the alpha/beta-interferon receptor gene usually is knocked out with insertion of the human CD46 gene).[28,40,41] In addition, in most of the CD46TG mice lines used in these studies, including in our present study, expression of human CD46 is driven by the human CD46 promoter, not the promoter of a ubiquitously expressed gene, leading to a pattern of CD46 expression similar to that in humans.[27,28,40] This conservation of the expression pattern

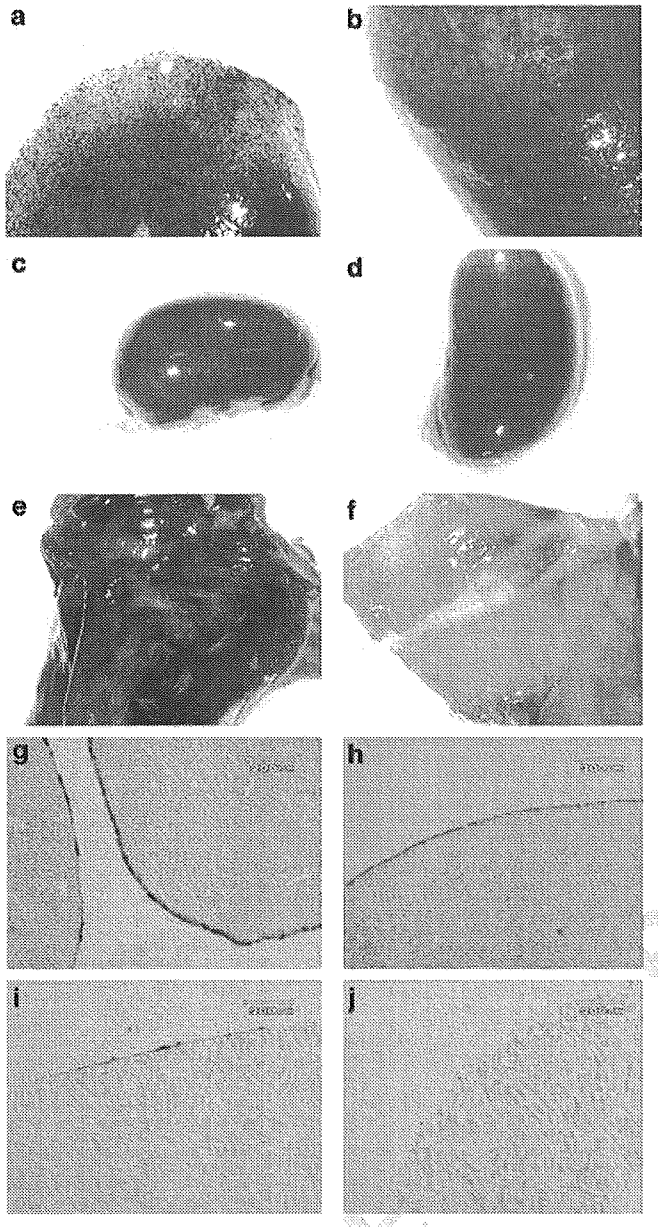

Figure 6 X-gal staining of the peritoneal organs of homozygous CD46TG mice receiving β-galactosidase-expressing Ad35 vectors. (**a**) Liver, (**c**) kidney, (**e**) peritoneum, (**g**) liver, and (**i**) kidney sections from homo TG mice injected with Ad35LacZ. (**b**) Liver, (**d**) kidney, (**f**) peritoneum, (**h**) liver, and (**j**) kidney sections from mock-infected homo TG mice. Ad35LacZ was injected intraperitoneally into homozygous CD46TG mice at a dose of 7.5×10^{10} VP/mouse. At 2 days postadministration, the organs were recovered after perfusion with 0.5% glutaraldehyde solution and then fixed and stained as described previously[54] by using 0.5% glutaraldehyde instead of 4% paraformaldehyde. For X-gal staining of liver and kidney, 10-μm sections were cut, fixed with 0.5% glutaraldehyde, and stained as described previously.[55]

is another advantage of using CD46TG mice as an animal model.

In vivo transduction experiments using CD46TG mice showed that Ad35 vectors mediated higher transduction efficiencies in CD46TG mice than wild-type mice, indicating that Ad35 vectors recognize human CD46 as an attachment receptor on *in vivo* application. However, the transduction efficiencies of Ad35 vectors in CD46TG mice were much lower than expected. Addition of human CD46 expression to mouse primary cells greatly enhanced Ad35 vector-mediated transduction (Figure 3). Our previous study demonstrated that the transduction activities of Ad5 and Ad35 vectors were nearly equivalent in human cultured cell lines,[13] which express high levels of CD46. These results suggest that, in cells expressing sufficient CD46, the transduction efficiencies of Ad35 vectors could be similar to those of Ad5 vectors. Therefore, we had expected that the transduction efficiencies of Ad35 vectors in CD46TG mice would greatly increase to levels comparable to those of Ad5 vectors. However, the transduction efficiencies of Ad35 vectors in the organs of homozygous CD46TG mice after intravenous administration were approximately 20- to 20000-fold lower than those of conventional Ad5 vectors at the same dose (1.5×10^{10} VP/mouse) in wild-type mice.[13] Why the *in vivo* transduction efficiencies of Ad35 vectors in CD46TG mice were lower than expected remains to be clarified. One possibility is that Ad35 vectors administered to CD46TG mice cannot access the human CD46 that is expressed on the cells. Human CD46 primarily is expressed on the basolateral surfaces of polarized epithelial cells,[42,43] and measles virus preferentially infects cells from their basolateral, rather than apical, sides.[44] Anatomical barriers such as the tightness between the basal membrane and extracellular matrix might impair the access of Ad35 vectors to the human CD46 on the basolateral cell surface. Another possibility is that an unidentified receptor or co-receptor for Ad35 is expressed in humans but not in CD46TG mice. Segerman *et al.* suggest that there are two different receptors in human cells for subgroup B Ads.[45] Interaction between Ad35 vectors and blood components (blood cells or serum proteins) also might inhibit Ad35 vector-mediated transduction after intravenous administration. In particular, the soluble form of human CD46, which is found in normal human serum,[46] might block infection by Ad35 vectors. However, preincubation of Ad35 vectors with serum or blood cells recovered from CD46TG mice did not reduce the transduction efficiencies of Ad35 vectors *in vitro* (data not shown). Further evaluation is necessary to clarify whether studies using CD46TG mice appropriately evaluate the transduction properties of Ad35 vectors. Currently, we are examining the transduction properties of Ad35 vectors in nonhuman primates, which express CD46 in all organs. The findings should greatly help us to understand characteristics of Ad35 vector-mediated transduction, including the validity and utility of CD46TG mice as model animals for Ad35 vectors.

The fiber shaft of Ad35 lacks the KKTK (Lys-Lys-Thr-Lys) motif, which is located in the fiber shaft of Ad5 and is considered to bind to heparan sulfate,[47] and its absence may partly explain the lower transduction efficiencies of Ad35 vectors than Ad5 vectors. Smith *et al.* demonstrated that amino acid substitution of the KKTK motif dramatically decreases the transduction efficiencies of Ad5 vectors in the mouse liver, whereas ablation of CAR- and integrin-binding sites did not significantly reduce in liver transduction with Ad5 vectors; these findings indicate a potential role for heparan sulfate binding in Ad5 vector-mediated liver transduction.[47] In addition, we reported that replacement of the Ad5 fiber shaft with the Ad35 shaft, in addition to the ablation of CAR and integrin binding, decreases Ad5 transduction efficiencies

NPG.GT.3302749

in the liver.[48] Heparan sulfate binding may be a more crucial determinant for Ad vector-mediated *in vivo* transduction of mice, especially in the liver, than binding to primary receptors (CAR for Ad5 and CD46 for Ad35), irrespective of Ad5 or Ad35 vectors.

Homozygous CD46TG mice, which express CD46 more abundantly than hemizygous CD46TG mice, seem to be more susceptible to Ad35 vectors than hemizygous mice (Figure 4). Our *in vitro* transduction experiments that used primary cells from CD46TG mice also demonstrated that mBM-DC and peritoneal macrophages derived from wild-type mice were refractory to Ad35 vectors, but high-level CD46 expression in cells from CD46TG mice increased the transduction efficiencies of Ad35 vectors (Figure 3). Together, these results indicate that CD46 expression levels are a crucial factor in Ad35 vector-mediated transduction. Anderson *et al.* reported a similar result, in which the transduction efficiencies of the chimeric Ad5F35 vector, which is an Ad5-based vector containing an Ad35 fiber shaft and knob, increased progressively with CD46 expression density in a panel of CHO cells stably expressing CD46.[49] Together, these findings suggest that Ad35 vectors can be a potent and selective platform for transduction into tumor cells expressing high levels of CD46, because human malignant tumor cells (including primary tumor cells) express CD46 more abundantly than nontransformed human cells.[23,24] Engineered measles viruses, which enter cells efficiently via CD46, exhibit selective oncolytic activity by exploiting the difference in CD46 expression levels between ovarian cancer cells and nontransformed cells.[23]

Transduction efficiencies of intraperitoneal administered Ad35 vectors were >10-fold higher in homozygous CD46TG mice than in wild-type mice (Figure 4). In particular, peritoneal organs, such as the liver, kidney, peritoneal wall, and diaphragm, were transduced efficiently. X-gal staining experiments demonstrated that efficient transduction occurred mainly in the mesothelial cells of the liver and kidney (Figure 6). In contrast, noteworthy luciferase production after intraperitoneal administration of Ad35 vector was not detected in the lung or heart, which are distant from the peritoneal cavity. Few LacZ-positive cells were found in the interior of the liver and kidney. These results indicate that after intraperitoneal injection, a portion of the Ad35 vector dose efficiently infects the mesothelia of tissues via CD46 on the surface of the organ, leading to efficient transduction. Another fraction of the dose, which probably is exuded into the bloodstream from the peritoneal cavity, likely poorly transduces the tissues of CD46TG mice. Using quantitative real-time PCR we confirmed that Ad35 vector DNA was present in the blood after intraperitoneal injection (data not shown).

In summary, we demonstrated that Ad35 vectors used the human CD46 expressed in CD46TG mice as an attachment receptor after *in vivo* administration. CD46TG mice are more susceptible to Ad35 vector-mediated transduction than wild-type mice, but the transduction efficiencies of Ad35 vectors in CD46TG mice were much lower than those of conventional Ad5 vectors.[13] As a next step, evaluation of Ad35 vector-mediated transduction in nonhuman primates, which ubiquitously express CD46 (as do humans), is necessary to assess the validity and utility of CD46TG mice as small animal models for Ad35 vectors.

Acknowledgements

We thank Ms Tomomi Sasaki, Ms Tsukasa Nakano, and Ms Kimiyo Akitomo for their technical assistance. We also thank Dr Naoki Okada (Kyoto Pharmaceutical University, Kyoto, Japan) for his help in preparation of bone marrow-derived dendritic cells. This work was supported by grants for Health and Labour Sciences Research from the Ministry of Health, Labour, and Welfare of Japan, and by Grants-in-Aid for Scientific Research on Priority Areas (B).

References

1 Havenga MJ, Lemckert AA, Ophorst OJ, van Meijer M, Germeraad WT, Grimbergen J *et al.* Exploiting the natural diversity in adenovirus tropism for therapy and prevention of disease. *J Virol* 2002; **76**: 4612–4620.

2 De Jong JC, Wermenbol AG, Verweij-Uijterwaal MW, Slaterus KW, Wertheim-Van Dillen P, Van Doornum GJ *et al.* Adenoviruses from human immunodeficiency virus-infected individuals, including two strains that represent new candidate serotypes Ad50 and Ad51 of species B1 and D, respectively. *J Clin Microbiol* 1999; **37**: 3940–3945.

3 Chirmule N, Propert K, Magosin S, Qian Y, Qian R, Wilson J. Immune responses to adenovirus and adeno-associated virus in humans. *Gene Ther* 1999; **6**: 1574–1583.

4 Stone D, Ni S, Li ZY, Gaggar A, DiPaolo N, Feng Q *et al.* Development and assessment of human adenovirus type 11 as a gene transfer vector. *J Virol* 2005; **79**: 5090–5104.

5 Smith TA, White BD, Gardner JM, Kaleko M, McClelland A. Transient immunosuppression permits successful repetitive intravenous administration of an adenovirus vector. *Gene Ther* 1996; **3**: 496–502.

6 Vlachaki MT, Hernandez-Garcia A, Ittmann M, Chhikara M, Aguilar LK, Zhu X *et al.* Impact of preimmunization on adenoviral vector expression and toxicity in a subcutaneous mouse cancer model. *Mol Ther* 2002; **6**: 342–348.

7 Rebel VI, Hartnett S, Denham J, Chan M, Finberg R, Sieff CA. Maturation and lineage-specific expression of the coxsackie and adenovirus receptor in hematopoietic cells. *Stem Cells* 2000; **18**: 176–182.

8 Tillman BW, de Gruijl TD, Luykx-de Bakker SA, Scheper RJ, Pinedo HM, Curiel TJ *et al.* Maturation of dendritic cells accompanies high-efficiency gene transfer by a CD40-targeted adenoviral vector. *J Immunol* 1999; **162**: 6378–6383.

9 Haviv YS, Blackwell JL, Kanerva A, Nagi P, Krasnykh V, Dmitriev I *et al.* Adenoviral gene therapy for renal cancer requires retargeting to alternative cellular receptors. *Cancer Res* 2002; **62**: 4273–4281.

10 Abrahamsen K, Kong HL, Mastrangeli A, Brough D, Lizonova A, Crystal RG *et al.* Construction of an adenovirus type 7a E1A-vector. *J Virol* 1997; **71**: 8946–8951.

11 Holterman L, Vogels R, van der Vlugt R, Sieuwerts M, Grimbergen J, Kaspers J *et al.* Novel replication-incompetent vector derived from adenovirus type 11 (Ad11) for vaccination and gene therapy: low seroprevalence and non-cross-reactivity with Ad5. *J Virol* 2004; **78**: 13207–13215.

12 Sakurai F, Mizuguchi H, Hayakawa T. Efficient gene transfer into human CD34+ cells by an adenovirus type 35 vector. *Gene Ther* 2003; **10**: 1041–1048.

NPG.GT.3302749

13 Sakurai F, Mizuguchi H, Yamaguchi T, Hayakawa T. Characterization of *in vitro* and *in vivo* gene transfer properties of adenovirus serotype 35 vector. *Mol Ther* 2003; **8**: 813–821.
14 Vogels R, Zuijdgeest D, van Rijnsoever R, Hartkoorn E, Damen I, de Bethune MP *et al.* Replication-deficient human adenovirus type 35 vectors for gene transfer and vaccination: efficient human cell infection and bypass of preexisting adenovirus immunity. *J Virol* 2003; **77**: 8263–8271.
15 Seshidhar Reddy P, Ganesh S, Limbach MP, Brann T, Pinkstaff A, Kaloss M *et al.* Development of adenovirus serotype 35 as a gene transfer vector. *Virology* 2003; **311**: 384–393.
16 Farina SF, Gao GP, Xiang ZQ, Rux JJ, Burnett RM, Alvira MR *et al.* Replication-defective vector based on a chimpanzee adenovirus. *J Virol* 2001; **75**: 11603–11613.
17 Reddy PS, Idamakanti N, Chen Y, Whale T, Babiuk LA, Mehtali M *et al.* Replication-defective bovine adenovirus type 3 as an expression vector. *J Virol* 1999; **73**: 9137–9144.
18 Nguyen T, Nery J, Joseph S, Rocha C, Carney G, Spindler K *et al.* Mouse adenovirus (MAV-1) expression in primary human endothelial cells and generation of a full-length infectious plasmid. *Gene Ther* 1999; **6**: 1291–1297.
19 Hofmann C, Loser P, Cichon G, Arnold W, Both GW, Strauss M. Ovine adenovirus vectors overcome preexisting humoral immunity against human adenoviruses *in vivo*. *J Virol* 1999; **73**: 6930–6936.
20 Gaggar A, Shayakhmetov DM, Lieber A. CD46 is a cellular receptor for group B adenoviruses. *Nat Med* 2003; **9**: 1408–1412.
21 Segerman A, Atkinson JP, Marttila M, Dennerquist V, Wadell G, Arnberg N. Adenovirus type 11 uses CD46 as a cellular receptor. *J Virol* 2003; **77**: 9183–9191.
22 Sakurai F, Kawabata K, Yamaguchi T, Hayakawa T, Mizuguchi H. Optimization of adenovirus serotype 35 vectors for efficient transduction in human hematopoietic progenitors: comparison of promoter activities. *Gene Ther* 2005; **12**: 1424–1433.
23 Peng KW, TenEyck CJ, Galanis E, Kalli KR, Hartmann LC, Russell SJ. Intraperitoneal therapy of ovarian cancer using an engineered measles virus. *Cancer Res* 2002; **62**: 4656–4662.
24 Bjorge L, Hakulinen J, Wahlstrom T, Matre R, Meri S. Complement-regulatory proteins in ovarian malignancies. *Int J Cancer* 1997; **70**: 14–25.
25 Tsujimura A, Shida K, Kitamura M, Nomura M, Takeda J, Tanaka H *et al.* Molecular cloning of a murine homologue of membrane cofactor protein (CD46): preferential expression in testicular germ cells. *Biochem J* 1998; **330** (Pt 1): 163–168.
26 Johnstone RW, Loveland BE, McKenzie IF. Identification and quantification of complement regulator CD46 on normal human tissues. *Immunology* 1993; **79**: 341–347.
27 Kemper C, Leung M, Stephensen CB, Pinkert CA, Liszewski MK, Cattaneo R *et al.* Membrane cofactor protein (MCP; CD46) expression in transgenic mice. *Clin Exp Immunol* 2001; **124**: 180–189.
28 Oldstone MB, Lewicki H, Thomas D, Tishon A, Dales S, Patterson J *et al.* Measles virus infection in a transgenic model: virus-induced immunosuppression and central nervous system disease. *Cell* 1999; **98**: 629–640.
29 Lemckert AA, Sumida SM, Holterman L, Vogels R, Truitt DM, Lynch DM *et al.* Immunogenicity of heterologous prime-boost regimens involving recombinant adenovirus serotype 11 (Ad11) and Ad35 vaccine vectors in the presence of anti-ad5 immunity. *J Virol* 2005; **79**: 9694–9701.
30 Barouch DH, Pau MG, Custers JH, Koudstaal W, Kostense S, Havenga MJ *et al.* Immunogenicity of recombinant adenovirus serotype 35 vaccine in the presence of pre-existing anti-Ad5 immunity. *J Immunol* 2004; **172**: 6290–6297.
31 Okada N, Masunaga Y, Okada Y, Iiyama S, Mori N, Tsuda T *et al.* Gene transduction efficiency and maturation status in mouse bone marrow-derived dendritic cells infected with conventional or RGD fiber-mutant adenovirus vectors. *Cancer Gene Ther* 2003; **10**: 421–431.
32 Takagi T, Kitano M, Masuda S, Tokuda H, Takakura Y, Hashida M. Augmented inhibitory effect of superoxide dismutase on superoxide anion release from macrophages by direct cationization. *Biochim Biophys Acta* 1997; **1335**: 91–98.
33 Mizuguchi H, Kay MA. Efficient construction of a recombinant adenovirus vector by an improved *in vitro* ligation method. *Hum Gene Ther* 1998; **9**: 2577–2583.
34 Mizuguchi H, Kay MA. A simple method for constructing E1- and E1/E4-deleted recombinant adenoviral vectors. *Hum Gene Ther* 1999; **10**: 2013–2017.
35 Zubieta C, Schoehn G, Chroboczek J, Cusack S. The structure of the human adenovirus 2 penton. *Mol Cell* 2005; **17**: 121–135.
36 Mizuguchi H, Koizumi N, Hosono T, Ishii-Watabe A, Uchida E, Utoguchi N *et al.* CAR- or alphav integrin-binding ablated adenovirus vectors, but not fiber-modified vectors containing RGD peptide, do not change the systemic gene transfer properties in mice. *Gene Ther* 2002; **9**: 769–776.
37 Wood M, Perrotte P, Onishi E, Harper ME, Dinney C, Pagliaro L *et al.* Biodistribution of an adenoviral vector carrying the luciferase reporter gene following intravesical or intravenous administration to a mouse. *Cancer Gene Ther* 1999; **6**: 367–372.
38 Huard J, Lochmuller H, Acsadi G, Jani A, Massie B, Karpati G. The route of administration is a major determinant of the transduction efficiency of rat tissues by adenoviral recombinants. *Gene Ther* 1995; **2**: 107–115.
39 Cattaneo R. Four viruses, two bacteria, and one receptor: membrane cofactor protein (CD46) as pathogens' magnet. *J Virol* 2004; **78**: 4385–4388.
40 Mrkic B, Pavlovic J, Rulicke T, Volpe P, Buchholz CJ, Hourcade D *et al.* Measles virus spread and pathogenesis in genetically modified mice. *J Virol* 1998; **72**: 7420–7427.
41 Johansson L, Rytkonen A, Bergman P, Albiger B, Kallstrom H, Hokfelt T *et al.* CD46 in meningococcal disease. *Science* 2003; **301**: 373–375.
42 Maisner A, Zimmer G, Liszewski MK, Lublin DM, Atkinson JP, Herrler G. Membrane cofactor protein (CD46) is a basolateral protein that is not endocytosed. Importance of the tetrapeptide FTSL at the carboxyl terminus. *J Biol Chem* 1997; **272**: 20793–20799.
43 Ichida S, Yuzawa Y, Okada H, Yoshioka K, Matsuo S. Localization of the complement regulatory proteins in the normal human kidney. *Kidney Int* 1994; **46**: 89–96.
44 Sinn PL, Williams G, Vongpunsawad S, Cattaneo R, McCray Jr PB. Measles virus preferentially transduces the basolateral surface of well-differentiated human airway epithelia. *J Virol* 2002; **76**: 2403–2409.
45 Segerman A, Arnberg N, Erikson A, Lindman K, Wadell G. There are two different species B adenovirus receptors: sBAR, common to species B1 and B2 adenoviruses, and sB2AR, exclusively used by species B2 adenoviruses. *J Virol* 2003; **77**: 1157–1162.
46 Seya T, Hara T, Iwata K, Kuriyama S, Hasegawa T, Nagase Y *et al.* Purification and functional properties of soluble forms of membrane cofactor protein (CD46) of complement: identification of forms increased in cancer patients' sera. *Int Immunol* 1995; **7**: 727–736.
47 Smith TA, Idamakanti N, Rollence ML, Marshall-Neff J, Kim J, Mulgrew K *et al.* Adenovirus serotype 5 fiber shaft influences *in vivo* gene transfer in mice. *Hum Gene Ther* 2003; **14**: 777–787.
48 Koizumi N, Mizuguchi H, Sakurai F, Yamaguchi T, Watanabe Y, Hayakawa T. Reduction of natural adenovirus tropism to mouse liver by fiber-shaft exchange in combination with both CAR- and alphav integrin-binding ablation. *J Virol* 2003; **77**: 13062–13072.
49 Anderson BD, Nakamura T, Russell SJ, Peng KW. High CD46 receptor density determines preferential killing of tumor cells by oncolytic measles virus. *Cancer Res* 2004; **64**: 4919–4926.

50 Kimura Y, Yanagimachi R. Intracytoplasmic sperm injection in the mouse. *Biol Reprod* 1995; **52**: 709–720.
51 Perry AC, Wakayama T, Kishikawa H, Kasai T, Okabe M, Toyoda Y *et al*. Mammalian transgenesis by intracytoplasmic sperm injection. *Science* 1999; **284**: 1180–1183.
52 Hosono T, Mizuguchi H, Katayama K, Xu ZL, Sakurai F, Ishii-Watabe A *et al*. Adenovirus vector-mediated doxycycline-inducible RNA interference. *Hum Gene Ther* 2004; **15**: 813–819.
53 Xu ZL, Mizuguchi H, Ishii-Watabe A, Uchida E, Mayumi T, Hayakawa T. Optimization of transcriptional regulatory elements for constructing plasmid vectors. *Gene* 2001; **272**: 149–156.
54 Sakai M, Nishikawa M, Thanaketpaisarn O, Yamashita F, Hashida M. Hepatocyte-targeted gene transfer by combination of vascularly delivered plasmid DNA and *in vivo* electroporation. *Gene Ther* 2005; **12**: 607–616.
55 Sakurai F, Nishioka T, Saito H, Baba T, Okuda A, Matsumoto O *et al*. Interaction between DNA-cationic liposome complexes and erythrocytes is an important factor in systemic gene transfer via the intravenous route in mice: the role of the neutral helper lipid. *Gene Ther* 2001; **8**: 677–686.

UNCORRECTED PROOF

Cancer Gene Therapy (2006) 00, 00–00
© 2006 Nature Publishing Group All rights reserved 0929-1903/06 $30.00
www.nature.com/cgt

ORIGINAL ARTICLE

Tumor suppressive efficacy through augmentation of tumor-infiltrating immune cells by intratumoral injection of chemokine-expressing adenoviral vector

N Okada[1], A Sasaki[1], M Niwa[1], Y Okada[2], Y Hatanaka[3], Y Tani[3], H Mizuguchi[4], S Nakagawa[5], T Fujita[1] and A Yamamoto[1]

[1]*Department of Biopharmaceutics, Kyoto Pharmaceutical University, Misasagi, Yamashina-ku, Kyoto, Japan;* [2]*Research Institute for Microbial Diseases, Osaka University, Suita, Osaka, Japan;* [3]*Department of Biomedical Science, DakoCytomation Company Ltd, Nishinotouin-higashiiru, Shijo-dori, Shimogyo-ku, Kyoto, Japan;* [4]*National Institute of Biomedical Innovation, Ibaraki, Osaka, Japan;* [5]*Department of Biopharmaceutics, Graduate School of Pharmaceutical Sciences, Osaka University, Suita, Osaka, Japan*

Our goal in the present study was to evaluate antitumor effects and frequency of tumor-infiltrating immune cells upon intratumoral injection of RGD fiber-mutant adenoviral vector (AdRGD) encoding the chemokines CCL17, CCL19, CCL20, CCL21, CCL22, CCL27, XCL1, and CX3CL1. Among eight kinds of chemokine-expressing AdRGDs, AdRGD-CCL19 injection most efficiently induced infiltration of T cells into established B16BL6 tumor parenchyma, whereas most of these T cells were perforin-negative in immunohistochemical analysis. Additionally, the growth of AdRGD-CCL19-injected tumors decreased only slightly as well as that of other tumors treated with each chemokine-expressing AdRGD, which indicated that accumulation of naive T cells in tumor tissue does not effectively damage the tumor cells. Tumor-bearing mice, in which B16BL6-specific T cells, were elicited by dendritic cell-based immunization, demonstrated that intratumoral injection of AdRGD-CCL17, -CCL22, or -CCL27 could considerably suppress tumor growth and attract activated T cells. On the other hand, AdRGD-CCL19-injection in the immunized mice showed slight increase of tumor-infiltrating T cells compared to treatment using control vector. Collectively, although AdRGD-mediated chemokine gene transduction into established tumors would be very useful for augmentation of tumor-infiltrating immune cells, a combinational treatment that can systemically induce tumor-specific effector T cells is necessary for satisfactory antitumor efficacy.
Cancer Gene Therapy (2006) **0,** 000–000. doi:10.1038/sj.cgt.7700903

Keywords: chemokine; adenoviral vector; tumor-infiltrating immune cell; melanoma

Introduction

Tumor cells that generally accumulate mutations in the genome express molecules different qualitatively and quantitatively from normal cells. An immunosurveillance system for these molecules, known as the tumor-associated antigen (TAA), plays an important role in the elimination of cancer cells during the initial stage.[1–3] However, because tumor cells are inherently autologous cells and their immunogenicity is very weak as compared with pathogens (non-self) invading from the outside world, malignant tumor cells can evade immunosurveillance and then infringe upon various biological functions by uncontrollable proliferation and metastasis. In addition, several soluble factors secreted from tumor cells are known to induce failure in the host's immune function.[4,5] Therefore, amelioration of illness exhibiting a growing tumor mass is difficult by innate immunity alone. Development of immunotherapy for cancer would involve the establishment of a methodology capable of enhancing recognition of tumor cell characteristics (differences from normal cells) by a patient's immune system, and accumulating activated immune effector cells at a local tumor site.

Cancer immunotherapy research has steadily progressed towards clinical application through cooperative fundamental research and clinical studies that have focused on adoptive transfer of lymphokine-activated killer cells or tumor-specific cytotoxic T lymphocytes (CTLs)[6,7] and administration of TAA-component vaccine,[8] TAA-coding DNA vaccine,[9] genetically modified tumor cell-based vaccine,[10,11] or TAA-delivered dendritic cell (DC)-based vaccine.[12–14] Although these approaches can induce and amplify tumor immunity in patients, satisfactory efficacy, including marked tumor regression or complete response, has not been previously reported in

Correspondence: Dr N Okada, Department of Biopharmaceutics, Kyoto Pharmaceutical University, 5 Nakauchi-cho, Misasagi, Yamashina-ku, Kyoto 607-8414, Japan.
E-mail: okada@mb.kyoto-phu.ac.jp
Received 27 April 2005; revised 11 July 2005; accepted 17 July 2005

Gml : Ver 6.0
Template: Ver 1.1.5

Journal: CGT ☐ Disk used Despatch Date: 24/9/2005
Article : npg_CGT_7700903 Pages: 13 Dimpleraj/Sudhir

a clinical setting. One potential cause of these disappointing results is insufficient investigation and understanding of methods that improve accumulation of immune effector cells in tumor tissue. The principal objective of most conventional studies of cancer immunotherapy has been efficient induction and activation of effector cells. Therefore, even if effector cells that exhibited the ability to kill tumor cells were adequately induced in a patient, the efficacy of cancer immunotherapy would be considerably limited if effector cells were unable to infiltrate tumor tissue and come in contact with tumor cells. Innovative approaches capable of better controlling biodistribution of immune effector cells are needed to overcome the limitations of current therapy.

Chemokine–chemokine receptor coupling controls leukocytic migration and infiltration of local sites through cooperation with various cell adhesion molecules.[15] Chemokines, which are small (8–14 kDa) secreted basic proteins, comprise a superfamily that contains four subgroups: C chemokine, CC chemokine, CXC chemokine, and CX3C chemokine.[16] These subgroups are defined by the position of conservative cysteine residues in the N-terminal and interactions with their specific receptors, which belong to the superfamily of seven-transmembrane domain G-protein-coupled receptors.[17,18] Initially, chemokines were identified as a group of cytokines capable of enhancing migration of neutrophils and monocytes, and functional analysis has focused on their role in inflammation. In the late 1990s, the sequence of immune chemokine, which primarily affects lymphocytes and DCs, was identified by a bioinformatics technique that used an EST database search. To date, more than 50 chemokines have been identified. Chemokines are now considered important molecules for cancer immunotherapy, which is based on the eradication of tumor cells as a consequence of interaction with immune cells that have migrated and accumulated in tumor tissues.[19–24]

We previously demonstrated that tumor cells transduced with RGD fiber-mutant adenoviral vector (AdRGD) encoding a chemokine gene could adequately secrete a biologically active chemokine, and that *in vitro* transfection established several chemokines as promising candidates for cancer treatment in three murine tumor models.[25,26] Although the inoculation of chemokine-transduced tumor cells was very useful for screening antitumor effects through the promotion of chemokine secretion in tumor tissue, direct *in vivo* injection of chemokine-expressing vector into tumor tissue is required for the development of effective chemokine-based cancer immunogenetherapy. Thus, in the present study, we attempted to investigate tumor suppressive effects of intratumoral injection of AdRGD encoding murine chemokines CCL17, CCL19, CCL20, CCL21, CCL22, CCL27, XCL1, and CX3CL1, and identify immune cells capable of infiltrating tumor tissue in the murine B16BL6 melanoma model.

Materials and methods

Cell lines and mice

HEK293 cells, the helper cell line for AdRGD propagation, were purchased from ATCC (Manassas, VA) and cultured in Dulbecco's modified Eagle's medium supplemented with 10% fetal bovine serum (FBS) and antibiotics. Murine melanoma B16BL6 cells (H-2^b) were obtained from JCRB cell bank (Tokyo, Japan) and grown in minimum essential medium supplemented with 7.5% FBS and antibiotics. EL4 cells, a T-lymphoma cell line of C57BL/6 origin, and YAC-1 cells, a lymphoma cell line highly sensitive to natural killer (NK) cells, were purchased from ATCC and maintained in RPMI 1640 medium supplemented with 10% FBS, 50 μM 2-mercaptoethanol, and antibiotics. Female C57BL/6 mice (H-2^b), age 7–8 weeks, were purchased from Japan SLC Inc. (Hamamatsu, Japan), and were held under specific pathogen-free conditions. Animal experimental procedures were in accordance with the Osaka University guidelines for the welfare of animals in experimental neoplasia.

Vectors

Replication-deficient AdRGD was based on the adenovirus serotype 5 backbone with deletions of E1 and E3 regions. The RGD sequence for αv-integrin-targeting was inserted into the HI loop of the fiber knob using a two-step method as previously described.[27] Eight murine chemokine-expressing AdRGDs (AdRGD-CCL17, -CCL19, -CCL20, -CCL21, -CCL22, -CCL27, -XCL1, and -CX3CL1),[25,26] gp100-expressing AdRGD (AdRGD-gp100),[28] and luciferase-expressing AdRGD (AdRGD-Luc)[27] were previously constructed by an improved *in vitro* ligation method.[27,29,30] All recombinant AdRGDs were propagated in HEK293 cells, purified by two rounds of cesium chloride gradient ultracentrifugation, dialyzed, and stored at −80°C. Titers of infective AdRGD particles (plaque-forming unit; PFU) were evaluated by the end point dilution method using HEK293 cells.

Generation and viral transduction of DCs

DCs were prepared according to the method of Lutz *et al*.[31] with slight modification. Briefly, bone marrow cells flushed from the femurs and tibias of C57BL/6 mice were seeded at $0.5–1 \times 10^7$ cells per sterile 100-mm bacterial grade culture dish in 10 ml of RPMI 1640 containing 10% FBS, 40 ng/ml recombinant murine granulocyte/macrophage colony-stimulating factor (kindly provided by KIRIN Brewery Co., Ltd, Tokyo, Japan), 50 μM 2-mercaptoethanol, and antibiotics. On day 3, another 10 ml of culture medium was added to the dish for medium replenishment. On day 6, 10 ml of the culture supernatant was collected and centrifuged at 1500 r.p.m. for 5 min at room temperature, and the pellet was resuspended in 10 ml of fresh culture medium, and then returned to the original dish to conserve unattached cells. On day 8, nonadherent cells were harvested and used as DCs. In transduction using AdRGD-gp100, DCs were suspended at a concentration of 5×10^6 cells/ml in FBS-

NPG.CGT.7700903

free RPMI 1640 and placed in a 50-ml conical tube. AdRGD-gp100 was added at 25 PFU/cell, the suspension was mixed well, and the tube was incubated at 37°C for 2 h with occasional gentle agitation. The cells were washed three times and resuspended with phosphate-buffered saline (PBS), and used in subsequent experiments as gp100/DCs.

Protocol for intratumoral injection of chemokine-expressing AdRGD (Protocol-1)

C57BL/6 mice were intradermally inoculated with 4×10^5 B16BL6 cells in the right flank. After 6 days, established tumors with diameters of 5–7 mm were injected with each vector at 3×10^8 PFU in 50-μl PBS.

Protocol for intratumoral injection of chemokine-expressing AdRGD in combination with gp100/DC immunization (Protocol-2)

B16BL6 cells were intradermally inoculated into C57BL/6 mice in the right flank at 4×10^5 cells/mouse. The next day, the mice were intradermally injected with 10^6 gp100/DCs in the left flank. Then, the 5–7 mm in diameter tumors were injected with each vector at 3×10^8 PFU in 50-μl PBS.

Evaluation of tumor growth

The major and minor axes of the tumors treated with Protocol-1 or -2 were measured using microcalipers, and tumor volume was calculated by the following formula: (tumor volume; mm^3) = (major axis; mm) × (minor axis; $mm)^2 \times 0.5236$. The mice were euthanized when one of the two measurements was greater than 20 mm.

Histopathological and immunohistochemical examination of tumor sections

Tumor-bearing mice were killed 2 days after the intratumoral injection of chemokine-expressing AdRGD in Protocol-1 or -2. For histopathological examination, the tumor nodules were harvested, placed in neutral 10% formalin/PBS, and embedded in paraffin. Sections (5 μm in thickness) were prepared for hematoxylin and eosin (HE) staining. For immunohistochemical analysis, the fresh tumor nodules were embedded in OCT compound (Sakura Finetechnical Co., Ltd, Tokyo, Japan), and frozen in liquid nitrogen. Frozen sections (5 μm in thickness) were fixed in 4% paraformaldehyde, washed with PBS, and then stored at −80°C until following immunostaining procedures. Only in the sections for Ki-67 detection, antigen retrieval treatment was performed with target retrieval solution pH6 (DakoCytomation Co., Ltd, Kyoto, Japan) at 95°C for 10 min. The immunostaining procedures, which included blocking for endogenous peroxidase activity with peroxidase blocking solution (DakoCytomation), blocking for nonspecific binding of the subsequently used immunoreagents with 5% bovine serum albumin, incubation with optimal dilution of antibody, incubation of reagent(s) for detection, and development with 3,3′-diaminobenzidine, were carried out on automated immunostaining system (Autostainer Plus, DakoCytomation). Between all incubation steps, the tumor sections were washed with Tris-bufferd saline containing Tween-20. The following antibodies were used as primary antibody; rat anti-mouse Ki-67 monoclonal antibody (mAb) (TEC-3; DakoCytomation), rat anti-mouse CD34 mAb (RAM34; BD Biosciences, San Jose, CA), rat anti-mouse F4/80 mAb (C1:A3-1; Serotec Co., Ltd, Sapporo, Japan), rabbit anti-human CD3 polyclonal antibody (DakoCytomation), rabbit anti-asialoGM1 polyclonal antibody (Wako Pure Chemical Industries, Ltd, Osaka, Japan), rat anti-mouse CD4 mAb (RM4-5; BD Biosciences), rat anti-mouse CD8 mAb (KT15; Serotec Co., Ltd), rat anti-mouse perforin mAb (P1-8; DakoCytomation), or hamster anti-mouse CD11c mAb (N418; CHEMICON International, Inc., Temecula, CA). Rat anti-mouse Ki-67 mAb was detected with biotinylated anti-rat Ig (DakoCytomation) and horseradish peroxidase (HRP)-conjugated streptavidin (DakoCytomation). Rabbit anti-human CD3 polyclonal antibody and rabbit anti-asialoGM1 polyclonal antibody were detected with ENVISION+ Rabbit/HRP (DakoCytomation). Hamster anti-mouse CD11c mAb was detected with HRP-conjugated anti-hamster Ig (BD Biosciences) and CSA II System (DakoCytomation). Other primary antibodies were detected with HRP-conjugated anti-rat Ig (Santa Cruz Biotechnology, Inc., Santa Cruz, CA) and CSA II System. The sections were finally counterstained with hematoxylin. The number of immunostained cells in six fields per specimen was counted under a light microscope using × 400 magnification.

Europium-release assay for cytolytic activity of CTLs

B16BL6 cells were intradermally inoculated into C57BL6 mice in the right flank at 4×10^5 cells/mouse. The next day, the mice were intradermally injected with 10^6 gp100/DCs or PBS in the left flank. At 1 week after immunization, nonadherent splenocytes were prepared from these tumor-bearing mice and restimulated *in vitro* using B16BL6 cells, which were cultured in media containing 100 U/ml recombinant murine interferon (IFN)-γ (PeproTech EC Ltd, London, UK) for 24 h and inactivated with 50 μg/ml mitomycin C at 37°C for 30 min, at an effector:stimulator ratio of 10:1 in RPMI 1640 supplemented with 10% FBS, 50 μM 2-mercaptoethanol, and antibiotics. After 5 days, the splenocytes were collected and used as effector cells. Target cells (IFN-γ-stimulated B16BL6, IFN-γ-stimulated EL4, and YAC-1 cell) were europium-labeled and a europium-release assay was performed as previously described.[32] Cytolytic activity was determined using the following formula: (% of lysis) = ((experimental europium-release − spontaneous europium-release)/(maximum europium-release − spontaneous europium-release)) × 100. Spontaneous europium-release of the target cells was < 15% of maximum europium-release by detergent.

NPG.CGT.7700903

Reverse transcription-polymerase chain reaction (RT-PCR) analysis of activation status of tumor-infiltrating immune cells

Tumors were collected 2 days after intratumoral injection in Protocol-1 and -2, and total RNA was isolated using Sepasol-RNA I Super (Nacalai Tesque, Inc., Kyoto, Japan), according to the manufacturer's instructions. RT proceeded for 60 min at 42°C in a 50 μl reaction mixture containing 5 μg total RNA treated with DNase I, 10 μl 5× RT buffer, 5 mM $MgCl_2$, 1 mM dNTP mix, 1 μM random primer (9-mer), 1 μM oligo$(dT)_{20}$, and 100 U ReverTra Ace (TOYOBO Co., Ltd, Osaka, Japan). PCR amplification of the perforin, granzyme B, IFN-γ, and β-actin transcripts was performed in 50 μl of a reaction mixture containing 1 μl of RT material, 5 μl 10× PCR buffer, 1.25 U *Taq* DNA polymerase (TOYOBO Co., Ltd), 1.5 mM $MgCl_2$, 0.2 mM dNTP, and 0.4 μM primers. The sequences of the specific primers were as follows: murine perforin: forward, 5′-ttt cgc ctg gta caa aaa cc-3′; reverse, 5′-cag tcc tgg ttg gtg acc tt-3′; murine granzyme B: forward, 5′-ctc gac cct aca tgg cct ta-3′; reverse, 5′-gaa agg aag cac gtt tgg tc-3′; murine IFN-γ: forward, 5′-gct ttg cag ctc ttc ctc at-3′; reverse, 5′-tga gct cat tga atg ctt gg-3′; murine β-actin: forward, 5′-tgt gat ggt ggg aat ggg tca g-3′; reverse, 5′-ttt gat gtc acg cac gat ttc c-3′. After denaturation for 2 min at 95°C, 20 cycles of denaturation for 30 s at 95°C, annealing for 30 s at 60°C (for perforin and β-actin) or 62°C (for granzyme B and IFN-γ), and extension for 30 s at 72°C were repeated and followed by completion for 4 min at 72°C. The PCR product was electrophoresed through a 3% agarose gel, stained with ethidium bromide, and visualized under ultraviolet radiation. EZ Load (Bio-Rad Laboratories, Inc., Tokyo, Japan) was used as a 100 bp molecular ruler. The expected PCR product sizes were 680 bp (perforin), 507 bp (granzyme B), 379 bp (IFN-γ), and 514 bp (β-actin).

Results

Growth and histology of B16BL6 tumor injected with chemokine-expressing AdRGD

In order to evaluate the suppressive effect of *in vivo* chemokine-gene transduction against established tumor, we investigated the changes in tumor volume after intratumoral injection of each chemokine-expressing AdRGD in murine B16BL6 melanoma model (Figure 1). Growth of B16BL6 tumor injected with AdRGD-Luc (control vector) at 3×10^8 PFU was equal to that of vehicle-injected tumor. On the other hand, mice injected intratumorally with each chemokine-expressing AdRGD exhibited slight delay of tumor growth as compared with control groups, and the rank order of the suppressive effect in eight chemokine-treated groups was CCL19 = CCL21 = CCL27 > CCL17 = CCL20 = CCL22-CX3CL1 > XCL1.

Next, histological changes of tumors injected with chemokine-expressing AdRGD were examined by HE staining (Figure 2a–d) and immunohistochemical staining against Ki-67 (a marker of proliferating cells; Figure 2e–h) and CD34 (a marker of vascular endothelial cells; Figure 2i–l). On day 2 after intratumoral injection, differences in frequency of granulocytic infiltration, size of necrotic area with undernourishment, proliferative state of tumor cells, and frequency of neovascularity were not observed among tumors injected with PBS, AdRGD-

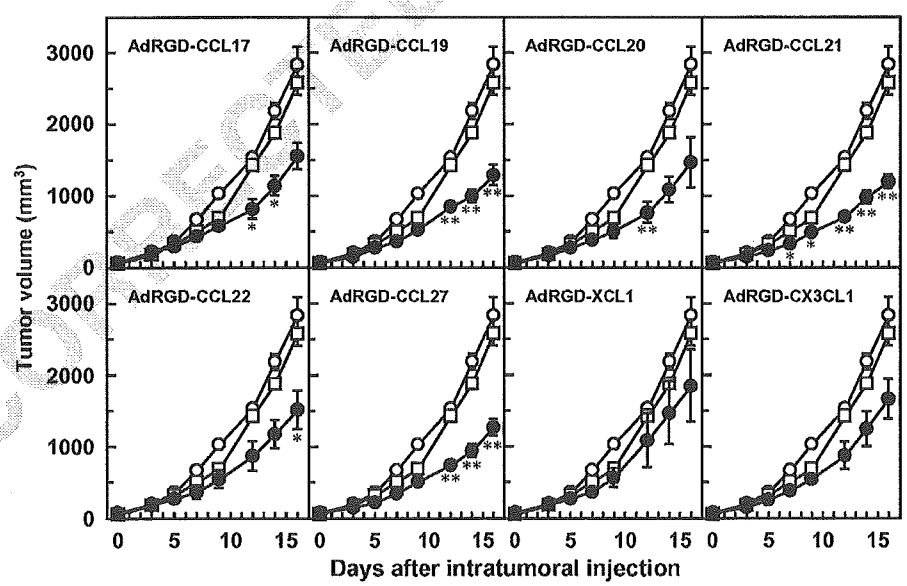

Figure 1 Anti-B16BL6 tumor efficacy of intratumorally injected chemokine-expressing AdRGD. B16BL6 cells were intradermally inoculated into the right flank of C57BL/6 mice at 4×10^5 cells/mouse. The tumors (5–7 mm in diameter) were injected with each chemokine-expressing AdRGD (●) or AdRGD-Luc (□) at 3×10^8 PFU. Likewise, PBS (○) was injected into the tumors. The tumor volume was calculated after measuring the major and minor axes of the tumor at indicated points. Each point represents the mean ± s.e. from 6 to 10 mice. Statistical analysis was carried out by Mann–Whitney *U*-test: $^*P<0.01$, $^{**}P<0.001$ versus AdRGD-Luc-injected group (□).

UNCORRECTED PROOF

NPG.CGT.7700903

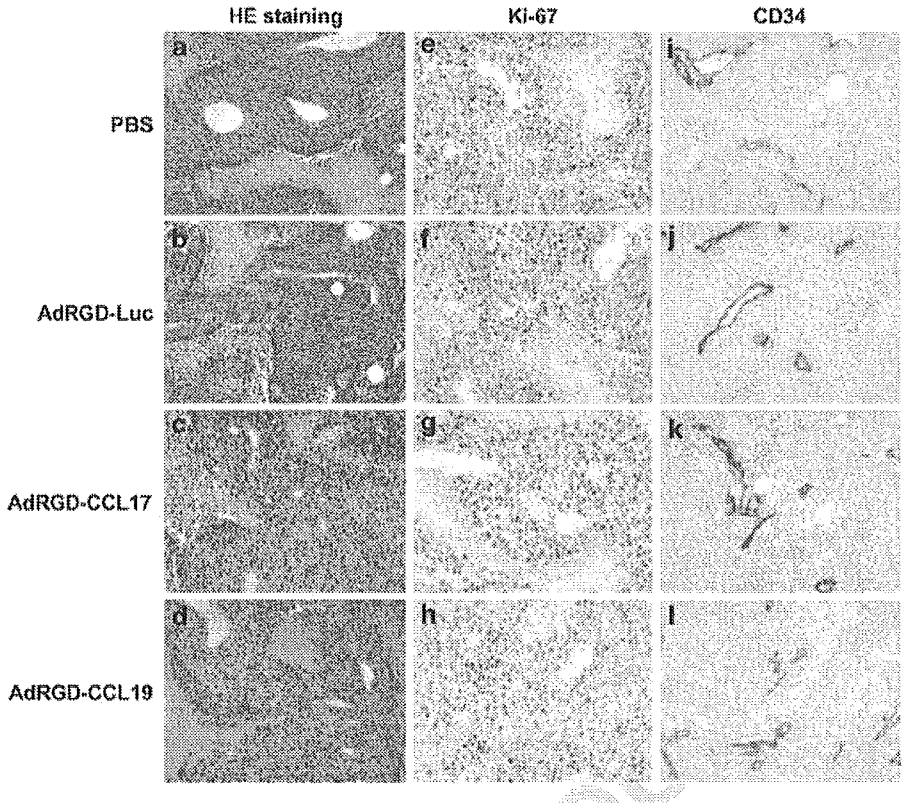

Figure 2 Histopathological and immunohistochemical examination of B16BL6 tumor injected with chemokine-expressing AdRGD. B16BL6 cells were intradermally inoculated into the right flank of C57BL/6 mice at 4×10^5 cells/mouse. The tumors (5–7 mm in diameter) were injected with AdRGD-Luc (**b**, **f**, **j**), AdRGD-CCL17 (**c**, **g**, **k**) or AdRGD-CCL19 (**d**, **h**, **l**) at 3×10^8 PFU. Likewise, PBS was administered into control tumors (**a**, **e**, **i**). On day 2 after intratumoral injection, HE staining (**a–d**) and immunohistochemical staining against Ki-67, to identify proliferating cells (**e–h**), and CD34, to identify vascular endothelial cells (**i–l**), were performed using paraffin-embedded tumor sections and frozen tumor sections, respectively. Original magnifications are $\times 200$.

Luc, AdRGD-CCL17, and AdRGD-CCL19. Similar pathological findings were also observed in other tumors treated with AdRGD-CCL20, -CCL21, -CCL22, -CCL27, -XCL1, or -CX3CL1 (data not shown). These observations revealed that AdRGD particle itself or the expressed chemokines did not contribute directly to injury of tumor cells and did not facilitate formation/breakdown of tumor vessels. Therefore, the data suggested that a delay in growth of B16BL6 tumor in response to direct injection of chemokine-expressing AdRGD might be caused by promotion of immune cell infiltration into tumor tissue by the secreted chemokines.

The subset and activation state of infiltrating immune cells in B16BL6 tumor injected with chemokine-expressing AdRGD

We attempted to identify the subset of infiltrating immune cells by immunohistochemical analysis in B16BL6 tumor 2 days after injection of chemokine-expressing AdRGD. In comparison with PBS-injected tumor, tumors injected with any AdRGD including control AdRGD-Luc exhibited increased F4/80-positive macrophage accumulation (Figure 3a–d), indicating that intratumoral administration of AdRGD induced inflammatory response in tumor tissue irrespective of the type of transgene. However, we determined that inflammation and macrophage-accumulation upon intratumoral injection of AdRGD would contribute little to the tumor suppressive effects induced by chemokine-expressing AdRGD because growth of B16BL6 tumor injected with AdRGD-Luc was comparable to that of PBS-injected tumor as shown in Figure 1. Notably, a large number of CD3-positive T cells were detected in tumors injected with AdRGD-CCL19, whereas T-cell accumulation in tumors injected with other chemokine-expressing AdRGD was moderately (AdRGD-CCL21), slightly (AdRGD-CCL17, -CCL20, -CCL22, and -CCL27), or not (AdRGD-XCL1 and -CX3CL1) different from that in control tumors (Figures 3e–h and 4a). In addition, subset analysis of the T cells that infiltrated the AdRGD-CCL19-injected tumor revealed that CCL19 induced significant infiltration of both $CD4^+$ and $CD8^+$ subsets, composed of helper T cells (Th) and CTLs, respectively, into tumor tissue (Figures 3m, n and 4a). However, most of these T cells attracted by CCL19 were not in a sensitized/activated state as demonstrated by the low amounts of perforin-positive cells in tumors injected with AdRGD-CCL19 (Figures 3o and 4a). Similarly, the perforin-positive cells were hardly recognized in tumors of several chemokine

NPG.CGT.7700903

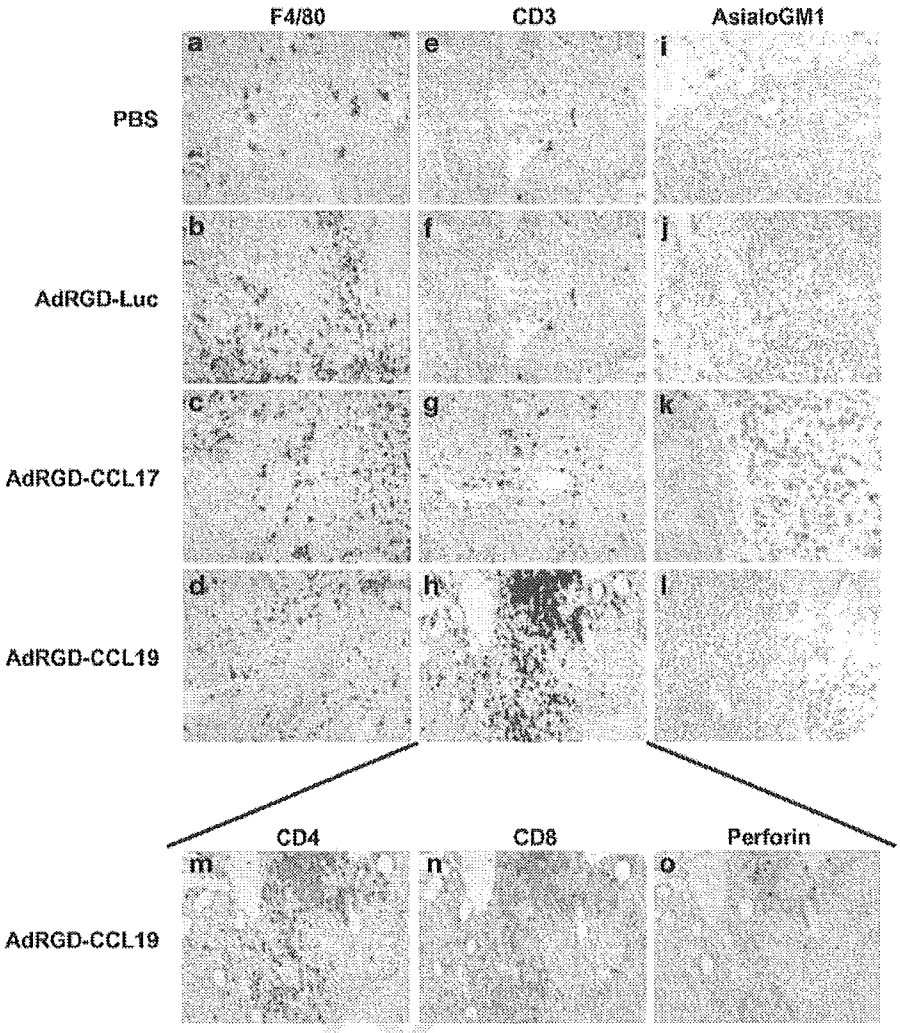

Figure 3 Infiltrating immune cell images in B16BL6 tumors injected with chemokine-expressing AdRGD. B16BL6 cells were intradermally inoculated into the right flank of C57BL/6 mice in at 4×10^5 cells/mouse. The tumors (5–7 mm in diameter) were injected with AdRGD-Luc (**b**, **f**, **j**), AdRGD-CCL17 (**c**, **g**, **k**), or AdRGD-CCL19 (**d**, **h**, **l**, **m**, **n**, **o**) at 3×10^8 PFU. Likewise, PBS was administered into control tumors (**a**, **e**, **i**). On day 2 after intratumoral injection, immunohistochemical staining against F4/80 (to detect macrophages; **a–d**), CD3 (for identification of T cells; **e–h**), and asialoGM1 (for identification of NK cells; **i–l**) was performed using frozen tumor sections. For determining the subset and the activation status of T cells in AdRGD-CCL19-injected tumor, immunohistochemical staining against CD4 (**m**), CD8 (**n**), and perforin (**o**) was performed using serial sections for H. Original magnifications are $\times 200$.

groups, which showed moderate increase of tumor-infiltrating $CD4^+$ and $CD8^+$ subsets (Figure 4a), indicating that intratumoral injection using our eight chemokine-expressing AdRGDs did not significantly attract activated effector cells that possessed potent killing activity against tumor cells. Considerable enhancement of NK cell-infiltration into parenchyma of tumor tissue was not observed in any groups injected with chemokine-expressing AdRGD (Figures 3i–l and 4a). On the other hand, intratumoral injection of AdRGD-CCL17 resulted in marked difference in the number of NK cells in the peritumoral portion as compared with the AdRGD-Luc-injected group, and moderate enhancement of NK cell-accumulation was observed at periphery of tumors injected with AdRGD-CCL19, -CCL21, or -CCL22 (Figures 3i–l and 4b). Immunostaining against CD11c showed that intratumoral injection of each chemokine-expressing AdRGD could not induce significant accumulation of DCs, which are the most potent antigen-presenting cells (Figure 4a).

Taken together, these data demonstrate that intratumoral injection of AdRGD-CCL19 drastically promotes T-cell infiltration into B16BL6 tumor tissue, and AdRGD-CCL17 injection most efficiently induces NK cell-accumulation at the peritumoral area, but not inside the tumor tissue. Moreover, perforin-positive immune cells were detected at extremely low levels in all tumors, suggesting that the tumor-infiltrating naive T cells attracted by chemokine gene transduction should be activated in tumor-specific manner in order to achieve more effective tumor elimination.

NPG.CGT.7700903

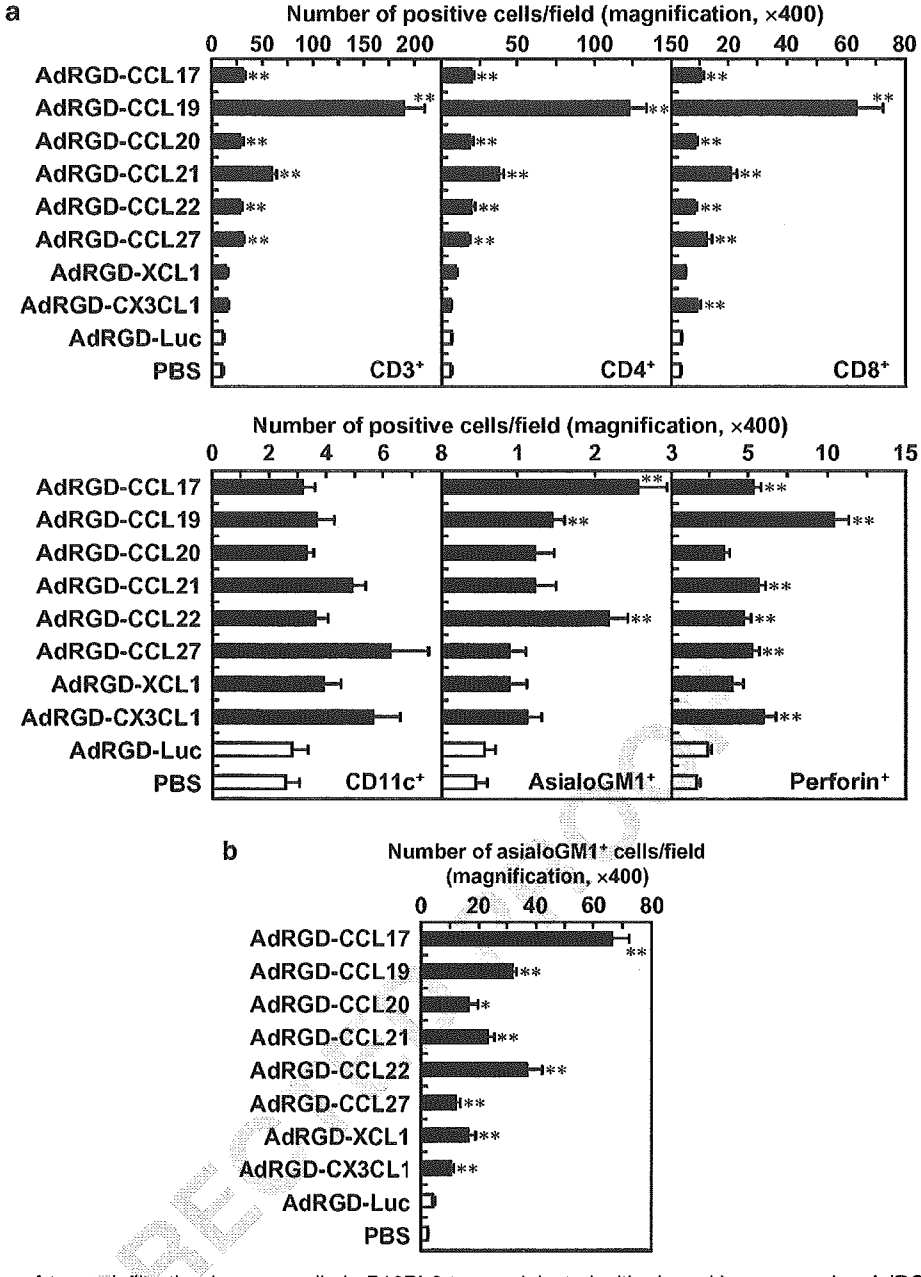

Figure 4 Identification of tumor-infiltrating immune cells in B16BL6 tumors injected with chemokine-expressing AdRGD. B16BL6 cells were intradermally inoculated into the right flank of C57BL/6 mice at 4×10^5 cells/mouse. The tumors (5–7 mm in diameter) were injected with each chemokine-expressing AdRGD or AdRGD-Luc at 3×10^8 PFU. Likewise, PBS was administered into control tumors. On day 2 after intratumoral injection, immunohistochemical staining against CD3, CD4, CD8, asialoGM1, perforin, and CD11c was performed using frozen tumor sections. Then, the number of positive cells in intratumoral (**a**) or peritumoral (**b**) sections was assessed by counting six fields per specimen under magnification × 400. The data represent the mean ± s.e. of results from three tumors. Statistical analysis was carried out by Welch's *t*-test: $^*P<0.01$, $^{**}P<0.001$ versus AdRGD-Luc-injected group.

Anti-B16BL6 tumor efficacy of combinational therapy using gp100/DC-immunization and intratumoral injection of chemokine-expressing AdRGD

We theorized that combination therapy, which includes a treatment that can activate tumor-specific immune response in the host, might be required for more effective application of chemokine-expressing AdRGD to cancer immunotherapy. We previously demonstrated that vaccination with DCs transduced with gp100, a melanoma-associated antigen, by using AdRGD could induce potent protective effects against murine B16BL6 melanoma challenge based on enhancement of gp100-specific CTL activity.[33] Thus, antitumor efficacy of a treatment combining intradermal immunization of gp100/DCs and intratumoral injection of chemokine-expressing AdRGD was investigated in B16BL6 tumor-bearing mice, according to the Protocol-2 described in the Materials and methods section.

In order to confirm the activation of systemic immunity in tumor-bearing mice immunized with gp100/DCs, we first evaluated CTL activity in splenocytes from these mice. Single immunization with gp100/DCs at a site distant from the tumor-inoculation site could promote killing activity of effector cells targeting B16BL6 cells (Figure 5a). As H-2 haplotype-matched irrelevant EL4 cells and YAC-1 cells, which are highly susceptible to NK activities, were not injured by these effector cells (Figure 5b and c), gp100/DC-administration could sensitize and activate gp100-specific CTLs in B16BL6 tumor-bearing mice as well as intact mice. As shown in Figure 6, mice injected intratumorally with PBS after gp100/DC-immunization did not exhibit considerable suppression of B16BL6 tumor growth as compared with unimmunized group, indicating that regression of B16BL6 tumor that had begun to proliferate was very difficult with only a single dose of gp100/DCs. At initial stage until day 11 after intratumoral injection, tumor growth in mice treated with AdRGD-Luc after gp100/DC-immunization was obviously delayed as compared with that in the PBS-injected group. We speculated that this suppressive effect was based on the activity of immune cells, including activated CTLs, which were attracted to tumor tissue by an inflammatory response to AdRGD-administration. In comparison with the control groups, AdRGD-CCL19 injection, which induced massive tumor-infiltrating T cells in unimmunized mice, only slightly delayed tumor growth in gp100/DC-immunized mice, although the effect was better than that by injection of AdRGD-CCL20 or -CCL21. Intratumoral injection of AdRGD-XCL1 or -CX3CL1 was not effective for promoting the tumor suppressive effect based on gp100/DC-immunization. On the other hand, intratumoral injection of AdRGD-CCL17, -CCL22, or -CCL27 in combination with gp100/DC-immunization could remarkably improve anti-

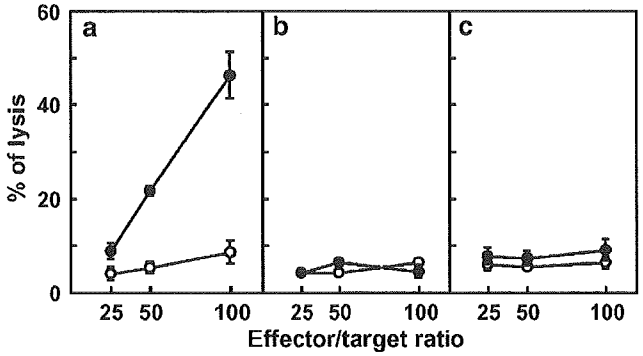

Figure 5 Enhanced tumor-specific CTL activity in B16BL6 tumor-bearing mice by gp100/DC-immunization. B16BL6 cells were intradermally inoculated into the right flank of C57BL/6 mice at 4×10^5 cells/mouse. One day later, the mice were intradermally injected with 10^6 gp100/DCs (●) or PBS (○) in the left flank. At 1 week after immunization, nonadherent splenocytes were prepared from these mice, and then were restimulated *in vitro* for 5 days with IFN-γ-stimulated and mitomycin C-inactivated B16BL6 cells. A cytolytic assay using the restimulated splenocytes was performed against IFN-γ-stimulated B16BL6 (**a**), IFN-γ-stimulated EL4 (**b**), and YAC-1 (**c**) cells. The data represent the mean±s.e. of three independent cultures from three individual mice.

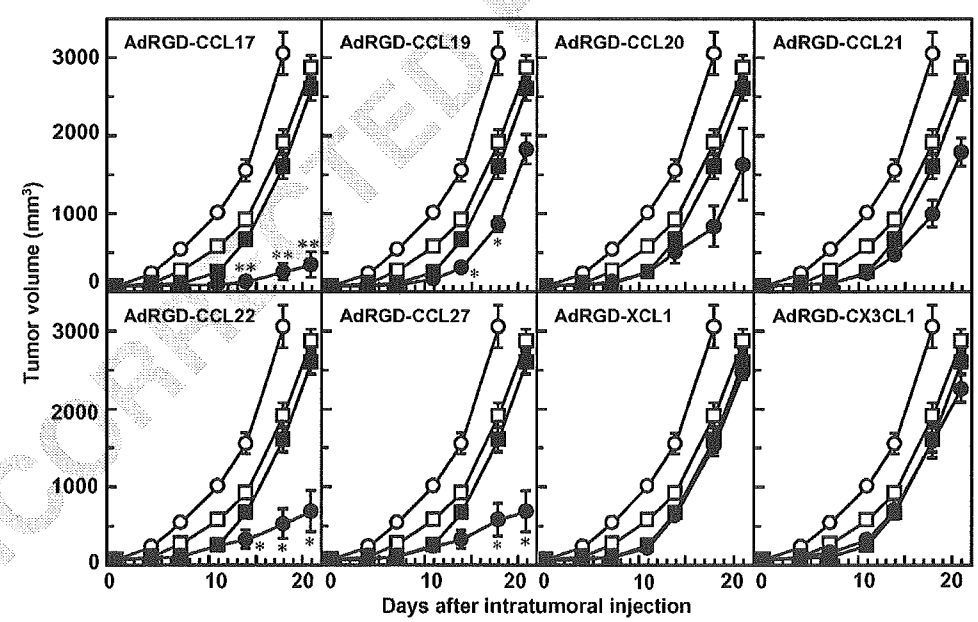

Figure 6 Anti-B16BL6 tumor efficacy of intratumorally injected chemokine-expressing AdRGD in combination with gp100/DC immunization. B16BL6 cells were intradermally inoculated into the right flank of C57BL/6 mice at 4×10^5 cells/mouse. The next day post-tumor inoculation, the mice were intradermally immunized with 10^6 gp100/DCs (●, ■, □) or PBS (○) in the left flank. Then, the tumors (5–7 mm in diameter) were injected with each chemokine-expressing AdRGD (●) or AdRGD-Luc (■) at 3×10^8 PFU. Likewise, PBS was administered into control tumors in mice pretreated with gp100/DCs (□) or PBS (○). Tumor volume was calculated after measuring the major and minor axes of the tumor at indicated points. Each point represents the mean±s.e. of 7–15 mice. Statistical analysis was carried out by Mann–Whitney *U*-test: $^*P<0.01$, $^{**}P<0.001$ versus AdRGD-Luc-injected group (■).

UNCORRECTED PROOF

NPG.CGT.7700903